Quaternary Science Reviews 305 (2023) 107992

Contents lists available at ScienceDirect

Quaternary Science Reviews

journal homepage: www.elsevier.com/locate/quascirev

Genesis and development of an interfluvial peatland in the central Congo Basin since the Late Pleistocene

Donna Hawthorne [a, *], Ian T. Lawson [a], Greta C. Dargie [b], Yannick E. Bocko [c], Suspense A. Ifo [d], Yannick Garcin [e], Enno Schefuß [f], William Hiles [a], Antonio Jonay Jovani-Sancho [g, h], Genevieve Tyrell [i], George E. Biddulph [a], Arnoud Boom [i], Brian M. Chase [j, k], Pauline Gulliver [l], Susan E. Page [i], Katherine H. Roucoux [a], Sofie Sjögersten [g], Dylan M. Young [b], Simon L. Lewis [b, m]

[a] School of Geography and Sustainable Development, University of St Andrews, St Andrews, Fife, KY16 9AL, UK
[b] School of Geography, University of Leeds, Leeds, LS2 9JT, UK
[c] Faculté des Sciences et Techniques, Université Marien Ngouabi, 99324, Brazzaville, Congo
[d] Ecole Normale Supérieure, Université Marien Ngouabi, 99324, Brazzaville, Congo
[e] Aix Marseille Univ, CNRS, IRD, INRAE, CEREGE, Aix-en-Provence, France
[f] MARUM—Center for Marine Environmental Sciences, University of Bremen, 28359, Bremen, Germany
[g] School of Biosciences, University of Nottingham, Loughborough, LE12 5RD, UK
[h] UK Centre for Ecology and Hydrology, Bangor, LL67 2UW, UK
[i] School of Geography, Geology & the Environment, University of Leicester, Leicester, LE1 7RH, UK
[j] Institut des Sciences de l'Evolution-Montpellier (ISEM), University of Montpellier, Centre National de la Recherche Scientifique (CNRS), EPHE, IRD, 34905, Montpellier, France
[k] Department of Environmental and Geographical Science, University of Cape Town, South Lane, Upper Campus, 7701, Rondebosch, South Africa
[l] NEIF Radiocarbon Laboratory, Scottish Universities, Environmental Research Centre, Glasgow, G75 0QF, UK
[m] Department of Geography, University College London, WC1E 6BT, UK

ARTICLE INFO

Article history:
Received 3 August 2022
Received in revised form
27 January 2023
Accepted 30 January 2023

Handling Editor: Giovanni Zanchetta

Keywords:
Palaeoecology
Pollen
Peat
Swamp
Tropical forest
Vegetation
Climate
Holocene
Congo Basin
Africa

ABSTRACT

The central Congo Basin contains the largest known peatland complex in the tropics. Here we present a detailed multi-proxy record from a peat core, CEN-17.4, from the centre of a 45 km wide interfluvial peatland (Ekolongouma), the first record of its kind from the central Congo peatlands. We use pollen, charcoal, sedimentological and geochemical data to reconstruct the site's history from the late Pleistocene to the present day. Peat began accumulating at the centre of the peatland ~19,600 cal BP (~17,500 −20,400 cal BP, 95% confidence interval), and between ~9500 (9430–9535 cal BP) and 10,500 (10,310 −10,660 cal BP) cal BP towards the margins. Pollen data from the peatland centre show that an initial grass- and sedge-dominated vegetation, which burned frequently, was replaced by a *Manilkara*-type dominated flooded forest at ~12,640 cal BP, replaced in turn by a more mixed swamp forest at ~9670 cal BP. Mixed swamp forest vegetation has persisted to the present day, with variations in composition and canopy openness likely caused at least in part by changes in palaeo-precipitation. Stable isotope data ($\delta D_{n\text{-}C29\text{-}v\&icecorr}$) indicate a large reduction in precipitation beginning ~5000 and peaking ~2000 cal BP, associated with the near-complete mineralization of several metres of previously accumulated peat and with a transition to a drier, more heliophilic swamp forest assemblage, likely with a more open canopy. Although the peatland and associated vegetation recovered from this perturbation, the strong response to this climatic event underlines the ecosystem's sensitivity to changes in precipitation. We find no conclusive evidence for anthropogenic activity in our record; charcoal is abundant only in the Pleistocene part of the record and may reflect natural rather than anthropogenic fires. We conclude that autogenic succession and variation in the amount and seasonality of precipitation have been the most important drivers of ecological change in this peatland since the late Pleistocene.

* Corresponding author.
E-mail address: dj43@st-andrews.ac.uk (D. Hawthorne).

https://doi.org/10.1016/j.quascirev.2023.107992

1. Introduction

The central Congo Basin (CCB), or Cuvette Centrale, spans parts of the Republic of Congo (ROC) and the Democratic Republic of Congo (DRC) (Fig. 1). This innermost part of the Congo Basin is dominated by forested wetlands (Bwangoy et al., 2010), large areas of which have recently been shown to have accumulated substantial thicknesses of peat (Dargie et al., 2017). The peatlands are estimated to occupy ~167,600 km^2 with a mean peat thickness of ~1.7 m and total carbon storage of ~29.0 Pg C, a substantial portion of the ~105 Pg C total peatland carbon storage in the tropics (Crezee et al., 2022).

Dargie et al. (2017) provided the first evidence for the age of the CCB peatland complex, reporting basal radiocarbon dates from nine locations in the northern CCB, all but one of which fell between ~10,550 and ~7140 cal BP (the outlier was a date of ~2160 cal BP). Dargie et al. proposed that a regional increase in rainfall during the African Humid Period (~14,800–5500 cal BP; deMenocal et al., 2000; Schefuß et al., 2005; Shanahan et al., 2015) may have facilitated waterlogging and hence peat initiation during the most humid part of the early Holocene.

Dargie et al. (2017) encountered peat consistently under three vegetation types: hardwood swamp forest (including *Uapaca mole* Pax, *Carapa procera* DC. and *Xylopia rubescens* Oliv.), and two types of palm-dominated swamp forest, one dominated by *Raphia laurentii* De Wild., and one much rarer type dominated by *R. hookeri* G. Mann and H. Wendl., which occurs in abandoned river channels. Previous studies elsewhere in the tropics have suggested that there are consistent relationships between vegetation type and 1) peat thickness, 2) nutrient availability, and 3) hydrological regime (i.e. degree and duration of flooding; e.g. Anderson, 1983, Anderson and Muller, 1975; Page et al., 1999; Llampazo et al., 2022). Since the build-up of peat over time at a site affects all of these factors, their interaction can lead to the development of complex spatio-temporal patterning of vegetation and other ecosystem properties over decadal to millennial timescales (e.g. Phillips et al., 1997; Roucoux et al., 2013; Kelly et al., 2020). Palaeoecological studies are central to identifying the relationships between vegetation, peat thickness, nutrient availability, and hydrology, all of which remain to be explored in the CCB.

Previous work on one of CCB peatlands, Ekolongouma (also the focus of the present study), found that it has a shallow domed surface, implying a largely rain-fed system (Dargie et al., 2017; Davenport et al., 2020). Various scenarios could account for the development of shallow peat domes in the CCB, including terrestrialisation of abandoned river channels or paludification of waterlogged floodplains followed by a later transition to ombrotrophy, but these hypotheses remain to be tested.

The peatland ecosystems of the CCB appear to be largely intact at the present day, at least in terms of hydrology and forest canopy cover, but they are vulnerable to anthropogenic pressures (Dargie et al., 2019). The communities living in and around the peatlands use various non-timber forest resources including fish, game, honey and fruit. Populations are concentrated in riverside settlements, including Bantu people who typically have a subsistence economy based on fishing and farming, and Aka and Twa *autochthon* (native or indigenous) communities who pursue, at least in part, a hunter-gatherer economy in CCB forests and swamps (Campbell, 2005; Olivero et al., 2016; Hewlett, 2017). Trails and in some places (but not, as far as we know, at our study site) narrow canals have been constructed to facilitate access to the swamp forest (Blake, 1993; Lewis, 2002). Expanding road networks and new pressures from oil exploration, logging, and commercial plantations could potentially damage the hydrological and ecological integrity of the peatlands and, inadvertently, lead to the release of stored peat carbon (Dargie et al., 2019). An understanding of past human impacts on the peatlands will help to contextualize the apparently low level of anthropogenic impact observed today and the potentially greater impacts that could accompany socio-economic development, if due care is not taken.

The CCB peatlands may also be vulnerable to 21st century climate change. The preservation and accumulation of peat, especially in ombrotrophic peatlands, requires the soil water table to be close to the surface for most of the year (e.g. Moore and Bellamy,

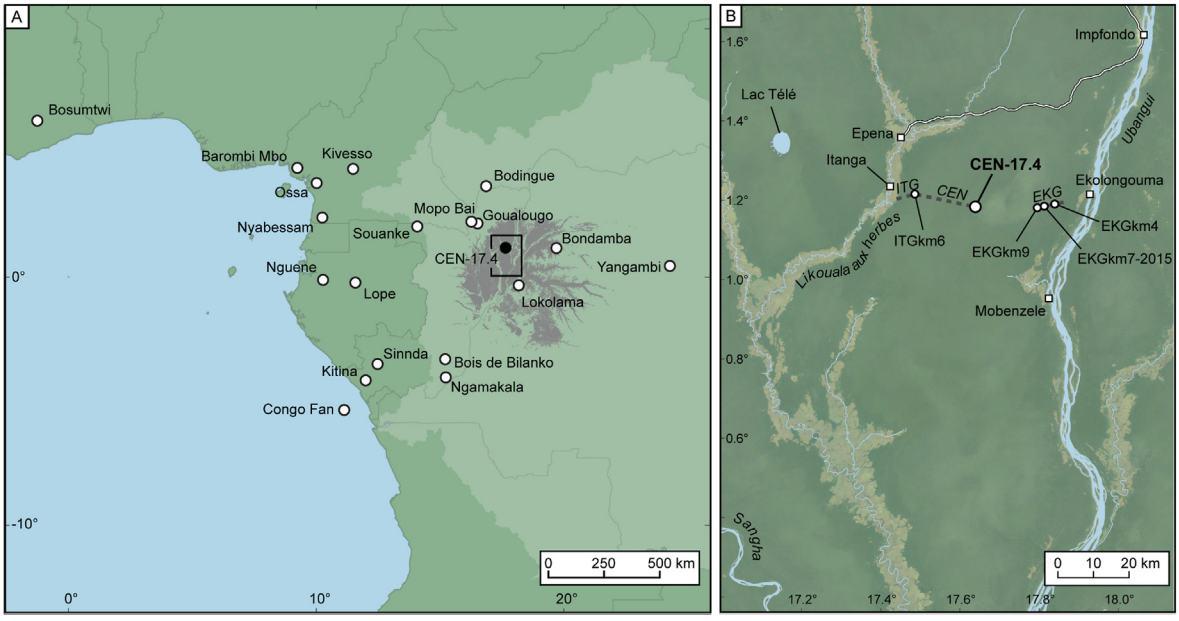

Fig. 1. Location of CCB peatlands (shown in grey), within the larger Congo hydrological basin (part shown, in light green) in Central Africa (panel A). Black rectangle shows location of panel B. Panel B shows the Likouala aux Herbes and Ubangui Inter-fluvial Basin, including the location of Transects (Itanga, Central and Ekolongouma), and the coring location (CEN-17.4 km). Additional sites mentioned in the text are labelled where appropriate in both panels.

1974; Page et al., 2006; Rydin et al., 2013; Cobb and Harvey, 2019). Water tables can be maintained by abundant rainfall and an absence of prolonged droughts. However, mean annual rainfall has declined in the region since 1979 and the boreal summer dry season has become more intense (Cook et al., 2020). A shift to drier conditions could lead to lowering of the water table, resulting in aerobic decomposition and mineralization of the peat (Hooijer et al., 2010; Dohong et al., 2017), releasing stored carbon to the atmosphere. Additionally, drying can leave the peat surface vulnerable to fire and to erosion via runoff, washing organic material into adjacent river systems (cf. Hemingway et al., 2017). Studies based on modelling and palaeoecological data from tropical peatlands outside Africa have suggested that future fluctuations in the intensity and pattern of rainfall could change the height and spatial distribution of water tables and increase the likelihood of peat surface drying (Hapsari et al., 2017; Leng et al., 2019). Palaeoclimatic data indicate that rainfall patterns in Central Africa have fluctuated throughout the Holocene (Schefuβ et al., 2005; Garcin et al., 2018); analysing the effects of these variations on past peat accumulation and other ecosystem properties will help to assess the potential impacts of future climate change.

To address the knowledge gaps identified above, here we present a detailed palaeoenvironmental proxy record from a peat core from the centre of the most intensively-studied peatland in the CCB, referred to here as the Ekolongouma peatland (informally named after an adjacent village; Fig. 1). The core, CEN-17.4, at 5.99 m, is the thickest peat sequence yet reported from the CCB. Here we use palynological and sedimentological data to describe and interpret the entire history of environmental change at the core site, from peat initiation to the development of the present-day domed, forested peat swamp. We use charcoal as a proxy for fire activity to assess the degree of past forest disturbance, and plant wax stable hydrogen isotopes as a proxy for precipitation to assess the influence of precipitation change on the peatland and vegetation over time. To place the CEN-17.4 record in context with the wider Ekolongouma peatland, we use published radiocarbon dates from four additional peat cores and peat depth measurements from three transects (Fig. 2), yielding insights into the spatio-temporal pattern and underlying processes of peat accumulation in this part of the CCB peatland complex.

1.1. Aims

1. Assess the spatio-temporal pattern of peat initiation and its subsequent accumulation and identify the likely drivers of these patterns.
2. Reconstruct past environments at the centre of the peatland from the late Pleistocene to the present day, particularly in terms of vegetation composition.
3. Assess the evidence for past human impacts on the peatland ecosystem.
4. Assess the effect of past climatic change on ecosystem properties at the site.

2. Site description

The CCB is thought to be underlain by 4–9 km of sediments ranging in age from Neoproterozoic to Neogene (Crosby et al., 2010; De Wit et al., 2015; Delvaux et al., 2021). The upper 1 km of these sediments are described as comprising Lower Cretaceous to Quaternary sediments (Kadima et al., 2011), likely deposited in fluvial, lacustrine and aeolian environments (De Wit et al., 2015). Dargie

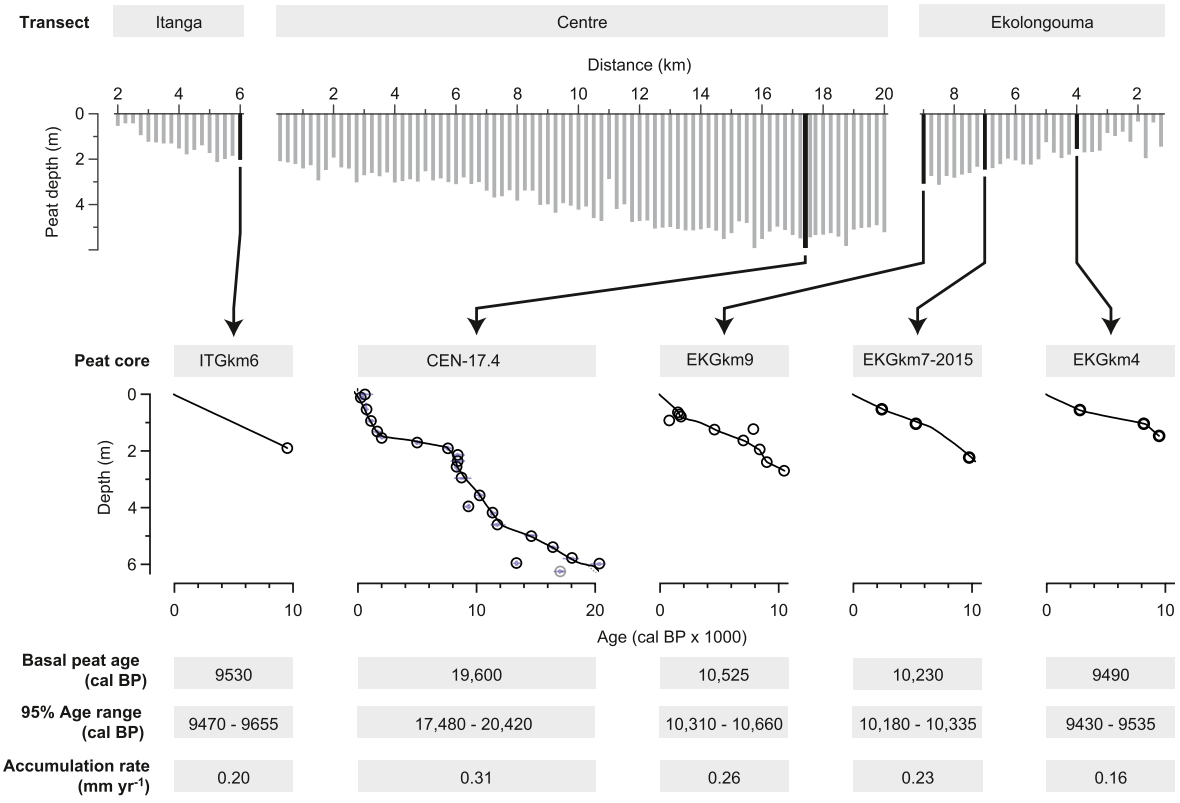

Fig. 2. Transect characteristics (Itanga, Centre and Ekolongouma). Peat depths (m) along each transect (distance, km, top panel), with peat core locations shaded in black. Corresponding radiocarbon chronologies for each peat core (middle panel), with basal dates, (median ages, cal BP; the basal peat date for CEN-17.4 is a central estimate from the age model (see section 4.1 for discussion)), associated age ranges (95%) and net accumulation rates (mm yr^{-1}) (bottom panel).

et al. (2017) and Crezee et al. (2022) have shown that these sediments are in turn overlaid in many places by several metres of largely Holocene peat.

The Ekolongouma peatland, the focus of the present study, is located in Likouala Department, Republic of Congo. The peatland is ~45 km wide from east to west, occupying an interfluve ~300 m above sea level between the southwards-flowing black-water Likouala-aux-Herbes and white-water Ubangui rivers. Three study transects (ITG, CEN and EKG; Fig. 1) together form a near-continuous transect across the interfluve from Itanga village in the west to Ekolongouma village in the east. The peat across the interfluve is underlain by clays and silts (Dargie, 2015). Peat thickness reaches a maximum of 5.99 m at the site of CEN-17.4, the main core studied here (Dargie, 2015). The peatland surface topography, reconstructed using LiDAR data, appears to increase in height from the peatland margin to the centre by ~1.8 m, indicating that the peatland is shallowly domed (Davenport et al., 2020).

Rainfall at the nearest meteorological station (Impfondo, ~1760 mm $y^{-1;}$ Samba et al., 2008) is low compared to some other tropical peatland regions (e.g. >3000 mm y^{-1} in Peruvian Amazonia; Marengo, 1998). There are two wet seasons each year, peaking in April/May and in October/November, and the intervening dry periods are short and rarely intense. The mean annual temperature is 25.6 °C with little variation throughout the year (Samba et al., 2008).

The vegetation at the core site is dominated by palms and hardwood trees (Fig. 3) including *R. laurentii*, *Carapa procera*, *Uapaca mole* and *Xylopia aethiopica* (Dunel) A. Rich.; the understorey is composed of *Aframomum* sp., Myristicaceae sp., Melastomataceae sp., *Palisota mannii* C. B. Clarke., *Pandanus candelabrum* P. Beauv., and ferns (Dargie, 2015). The canopy at the coring site is lower and more open than along the rest of the CEN transect (Dargie et al., 2017). Two end-member vegetation types were described, hardwood swamp forest at the western end and *R. laurentii*-dominated palm swamp at the eastern end of the CEN transect, with gradual variation in the relative proportions of hardwood trees and palms in between (Dargie, 2015).

3. Methodology

3.1. Peat sampling and peat depth

'Peat' is defined here as material with loss-on-ignition (LOI) > 65%, following Dargie et al. (2017). The peat core analysed in this study was retrieved in March 2014 at 01.1835°N, 017.6399°E. The core was taken with a 5 cm diameter, 50 cm long Russian-type corer in 13 overlapping sections in two parallel holes to a depth of 6.29 m, coring past the base of the peat (5.99 m) into the underlying clays which prevented further sampling. Each section was wrapped, transported under licence to the UK and refrigerated at 4 °C. The entire core was sub-sampled in the laboratory at 4 cm resolution for isotopic analysis and up to 2 cm resolution (including analytical intervals of 16, 8 and 4 cm) for palaeoecological analysis. Sampling for testate amoebae and plant macrofossils was carried out but preservation was too poor to allow analysis. Where necessary, depths were corrected using linear interpolation to account for up to 5 cm of compaction during transportation from the core site. Additional peat cores from the Itanga and Ekolongouma transects were collected and studied by Dargie (2015). Peat thickness was measured at 250 m intervals along the transects by probing the peat with a pole (Dargie, 2015).

3.2. Radiocarbon dating and age model construction

Twenty-two bulk peat samples from core CEN-17.4, sieved at 150 μm to remove roots as far as possible, were dated by radiocarbon AMS analysis at the Alfred Wegener Institute and first published by Garcin et al. (2022). Dates from four other cores (ITGkm6, EKGkm9, EKGkm7-2015, EKGkm4) along the Ekolongouma and Itanga transects were previously published by Dargie et al. (2017). All dates were recalibrated for this analysis using a 50:50 mix of the IntCal20 and SHCal20 calibration curves (Hogg et al., 2020) in the *IntCal* package in *R* v. 4.0.3 (R Core Team, 2021); for brevity, ages cited in the text are median calibrated ages unless otherwise stated. Radiocarbon dates are presented in full in Appendix A. The age model for CEN-17.4 was constructed using the *R* package *rBacon* v.2.5.8 (Blaauw and Christen, 2011), setting the priors to allow for low memory and a wide range of accumulation rates (acc.mean = 40, acc. shape = 1, mem. mean = 0.1, ssize = 15,000, mem. strength = 2). The resulting age model places little weight on three samples (at 396, 596 and 625 cm) that returned ages substantially younger than adjacent dates. This is a common occurrence, particularly in the dating of slow accumulating basal peats and can be due to a number of factors e.g. downward penetration of roots and/or contamination during coring (Quik et al., 2022).

3.3. Palynology

Pollen preparation followed conventional methods (Moore et al., 1991), substituting density separation (Nakagawa et al., 1998) for HF treatment. Two *Lycopodium* tablets (Lund University

Fig. 3. Two vegetation types present along the Ekolonouma transect, hardwood swamp forest (left) and palm-dominated swamp forest (right).

batch no. 201890, 11,267 ± 370 spores per tablet) were used as an exotic marker in each 1 cm^3 sample of peat. Samples were mounted in silicone oil and routinely counted and identified at ×1000 magnification using a Zeiss Axioskop microscope. Identifications were made using a pollen key derived from reference material compiled from the literature and personal observations and/or photographs from reference collections at the University of Oxford, Institute of Archaeological Sciences, Goethe University Frankfurt, Institute of Evolutionary Science of Montpellier, University of Montpellier II, and collections held by the National Museum of Paris and accessed through LOCEAN at Pierre and Marie Curie University Paris. Pollen identifications were made to the lowest taxonomic level possible, either family (listed as e.g. Poaceae or Cyperaceae), genus (listed as e.g. *Raphia*) or species level (listed as e.g. *Symphonia globulifera* L. f.). Pollen grains have been listed as a 'type', e.g. *Alisma*-type, when it is clear that other genera produce identical pollen. The incomplete state of pollen taxonomy in central Africa means that any of these identifications and attributions may include other genera or species whose pollen has not yet been described in the literature. Samples were counted to a minimum sum of 300 grains, including arboreal and herbaceous pollen. Spores were excluded from the pollen sum (and calculated as a percentage outside of the pollen sum), but the sum does include unidentified morphotypes, which make up less than 5% of the assemblages. Palaeoecological interpretations are based primarily on ecological information from the African Plant Database v. 3.4.0 and on vegetation census data from the Ekolongouma site, supplemented by information in the palaeoecological and ecological literatures (e.g. Elenga et al., 2000; Brncic et al., 2007; Kiahtipes et al., 2011; Moutsamboté, 2012; Ifo et al., 2016: Bocko et al., 2016); see section 5.2 for further discussion.

3.4. Palynological data analysis

Pollen assemblage zones were defined using stratigraphically constrained cluster analysis, a Bray-Curtis dissimilarity matrix and the CONISS method, including only taxa achieving >5% abundance in at least one sample (Birks and Gordon, 1985). The choice of number of zones (five) was informed by a broken stick model (Bennett, 1996) and visual examination of key vegetation transitions in the pollen data. Indicator species analysis (Dufrêne and Legendre, 1997) was performed to determine which taxa were characteristic of each zone, referred to here as indicator taxa. As an aid to discussion, additional subzones were defined using the cluster analysis as a guide; one additional subzone boundary (at 180 cm) was added to facilitate comparison with the other proxy data. To further inform our interpretation of the structure of the dataset, non-metric multidimensional scaling (NMDS) ordination (Legendre and Birks, 2012) was carried out on the same dissimilarity matrix. In order to highlight associations between individual taxa throughout the dataset, we applied a correlated topic model (CTM; Blei and Lafferty, 2007), based on taxon abundances, to the same subset of pollen data. This method, only recently applied in palaeoecology, identifies sets of taxon associations within a dataset, allowing one taxon to characterise more than one association, which allows for the overlapping species associations found in nature. Finally, rarefied richness was used to estimate palynological diversity. These analyses were carried out in *R* using the *labdsv* (v. 2.0–1, Roberts, 2019), *rioja* (v. 0.9–26, Juggins, 2020), *stm* (v. 1.3.6, Roberts et al., 2019) and *vegan* (v. 2.6–2, Oksanen et al., 2020) packages.

3.5. Sedimentology

LOI analysis was carried out on 1 cm^3 sub-samples at 550 °C for 4 h following Heiri et al. (2001). Particle size analysis was carried out on the lowermost peat and underlying sediments, below 550 cm, using a Beckman Coulter LS230 Particle Size Analyser (Goossens, 2008) on 1 cm^3 sub-samples which had been digested in 30% H_2O_2 then 10% HCl to remove organic matter and carbonates.

3.6. Organic geochemistry

Total organic carbon (TOC), total nitrogen (TN), and $\delta^{13}C_{TOC}$ were measured on bulk samples, and stable isotope ratios (D:H and ^{13}C:^{12}C) were measured on C_{29}-alkanes extracted from the peat. $\delta D_{n\text{-}C29}$ values (Garcin et al., 2022) reflect variations in the isotopic composition of precipitation representing changes in past precipitation regimes, i.e. the amount and seasonality of precipitation (Sachse et al., 2012; Ladd et al., 2021). $\delta D_{n\text{-}C29}$ is negatively correlated with precipitation amount in Central Africa (Collins et al., 2013; Garcin et al., 2018). As these isotopic values can be influenced by vegetation type (Sachse et al., 2012) and global ice volume (Waelbroeck et al., 2002), we corrected for both vegetation and ice volume here (not applied in Garcin et al., 2022), i.e. $\delta D_{n\text{-}C29\text{-}v\&icecorr}$ (Collins et al., 2013; Feakins, 2013; Shanahan et al., 2015; Tierney et al., 2017; Garcin et al., 2018). The organic geochemistry data were further compared with the previously acquired I-index, which is derived from Rock-Eval® analysis (Garcin et al., 2022). The I-index relates to the ratio between the thermally labile and resistant pools of organic matter (Sebag et al., 2016). Further methodological details are given in Appendix B.

3.7. Inorganic geochemistry

The concentrations of major elements were analysed by Inductively Coupled Plasma Mass Spectrometry (ICP-MS). Peat samples were dried at 65 °C, milled, and digested in HNO_3 then H_2O_2 before analysis. Further methodological details are given in Appendix B.

3.8. Microscopic and macroscopic charcoal

Microscopic charcoal fragments (>10 μm) (representing regional fire activity) were quantified at the time of pollen counting using the pollen-slide method (Clark, 1988). Macroscopic charcoal fragments (>125 μm) (representing local fire activity) were extracted from 1 cm^3 subsamples by sieving, bleaching, and disaggregation using 40 ml 15% $Na_6P_6O_{18}$ to disaggregate organic matter, following Hawthorne et al. (2018). Macroscopic charcoal fragments were counted and measured using digital image analysis (ImageJ software: Abràmoff et al., 2004). The macroscopic records of charcoal area *vs* number were compared, confirming that particle breakage was not an issue during processing.

4. Results

4.1. Peat thickness, basal peat age and long-term net accumulation rate

The maximum peat thickness across all transects, 5.99 m, was recorded at the site of core CEN-17.4 (Fig. 1), close to the centre of the interfluve. Peat thickness decreases towards the margins of the basin (Fig. 2). Small-scale variations in peat thickness along each transect likely reflect both surface microtopographic variation (undulations <1 m were observed in the field) and unevenness in the underlying substrate.

Our age-depth model (Fig. 4) yields central age estimates for the base of CEN-17.4 at ~20,400 cal BP (~22,000–18,050 cal BP, 95% confidence interval), with peat initiation (at 599 cm) estimated at

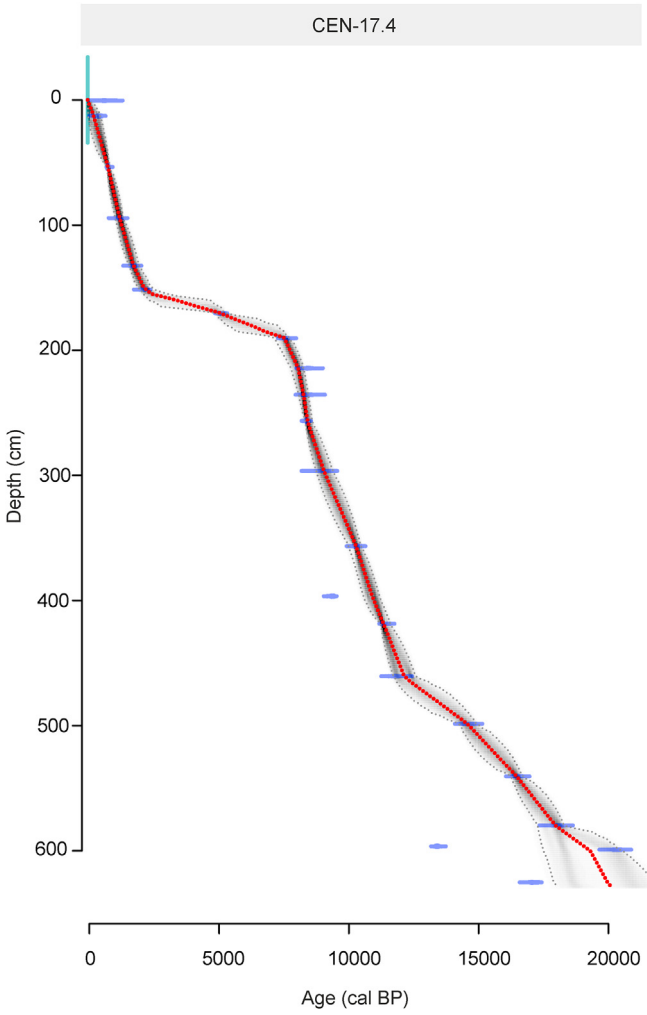

Fig. 4. Age-depth model for core CEN-17.4, modelled in rbacon v.2.5.8 (Blaauw and Christen, 2011) using a mixed calibration curve (50:50 mix of the IntCal20 and SHCal20 (Hogg et al., 2020) in the *IntCal* package in *R* v. 4.0.3 (R Core Team, 2021).

~19,600 cal BP (~20,400–17,500 cal BP, 95% confidence interval). These age estimates should be treated with caution because two of the dates near the base (at 596 and 625 cm) are out of stratigraphic sequence (younger than surrounding dates). It would be possible, though less parsimonious, to construct an age model that placed more weight on the dates at 596 and 625 cm, which would give a younger date for peat initiation, closer to ~17,500 cal BP; or alternatively to yield a slightly older estimate for peat initiation by placing more weight on the date at 599 cm, which calibrates to ~20,100–20,500 cal BP (95% confidence interval).

Peat initiation dates from the other cores at the site are considerably younger, dating to the early Holocene and showing a trend of decreasing age from the centre to the edge of the site, with median ages of 10,525 cal BP at EKGkm9, 10,230 cal BP at EKGkm7-2015, and 9490 cal BP at EKGkm4, to the east of CEN-17.4; and 9530 cal BP at ITGkm6, to the west (Fig. 2).

The long-term net peat accumulation rate at CEN-17.4 is 0.31 mm y^{-1}. Net long-term peat accumulation rates for cores EKGkm9, EKGkm7-2015, EKGkm4 and ITGkm6 are 0.26, 0.23, 0.16 and 0.20 mm yr^{-1} respectively, declining systematically from the centre towards the edge of the site. These figures, however, mask considerable stratigraphic variation evident in the shape of the age-depth models (Figs. 2 and 4). Age-depth curves may not represent the net accumulation rate that occurred at the time of peat formation because of subsequent decomposition (Young et al., 2021), and additional proxy evidence (discussed below) is needed to fully understand how peat carbon storage has changed over time. However, an important feature of CEN-17.4 is the substantial change in the age-depth relationship between 190 and 151 cm (~7500–2000 cal BP). The depth/age gradient here is 5–8 times lower than in the rest of the sequence. This stratigraphic feature was termed the 'Ghost Interval' by Garcin et al. (2022), who interpreted it as representing a section of peat that has largely been lost due to enhanced contemporaneous and secondary decomposition during a dry interval from ~5000 to 2000 cal BP. The age-depth models for additional cores from Ekolongouma with multiple dates all show a similar feature in the mid-Holocene, though less well defined perhaps due simply, to the lower density of dates (Fig. 2).

4.2. Palaeoenvironmental proxy data from CEN-17.4

The palynological analysis of CEN-17.4 yielded 155 taxa of which 24 are unidentified morphotypes, never totalling more than 5% of the assemblages. Taxa achieving >5% abundance in at least one sample are plotted in Fig. 5. Pollen preservation was generally excellent throughout the core. The pollen assemblage zones provide a convenient stratigraphic framework within which to describe the other proxy data. The proxy data are presented in detail in Table 1. For brevity, in the text below we describe only the most important features of the palaeo-proxy record.

The 629 cm-long sequence consists of fine clayey silts below 599 cm, with a sharp transition to peats at this depth; LOI and TOC data (Fig. 8) indicate that the ash content of the peat continues to decline slowly throughout the remainder of Zones I and II. Palynologically, several taxa are present throughout the entire record, including *Pycnanthus*, *Macaranga*, *Syzygium*, *Lophira*, *Raphia* and *Pandanus*. Overlying this picture of continuity are some systematic long-term changes, notably a gradual increase in the abundance of *Raphia, Pandanus* and *Symphonia globulifera* over time, reflected in the general trend of the samples from positive to negative NMDS axis 1 scores (Fig. 6). There is also a lot of high-frequency variation: in detail, the relative abundances of these taxa rarely remain constant for long. Zones I and II are defined by distinctive palynological assemblages, but Zones III to V vary mainly in the relative abundances of a consistent set of taxa.

Zone I (20,400–12,650 cal BP) extends from the base of the sequence to its upper boundary at 12,650 cal BP. The palynology of this zone is dominated by herbs, notably Cyperaceae and Poaceae, and the aquatic *Alisma*-type. Zone I is divided into five subzones which reflect an oscillation between a dominance of herbs (Subzones Ia, c, e) and trees including *Pycnanthus*, *Macaranga*, *Syzygium*, *Lophira*, *Raphia* and *Pandanus* (Subzones Ib, d). Micro- and macro-charcoal are abundant throughout Zone I, covarying with Cyperaceae and Poaceae. No diatoms or other siliceous microfossils were observed in the basal sediments (below 599 cm, within Subzone Ia), which are unlaminated Al-rich clayey silts with a median particle size ranging from 4 to 6 μm; *Alisma*-type is also absent from these basal sediments. The organic geochemistry of the peat in Zone I (above 599 cm) is variable with generally very positive $\delta^{13}C_{Bulk}$ values and low C/N, markedly different from the peats in Zones II–V. The inorganic geochemistry (Fig. 9) of this Zone I peat is also distinct from the peat in other zones, being proportionately rich in Al, Ti, Pb, P and Cu especially in Subzone Ic where the peat LOI values show a marked dip.

Zone II (12,650–9680 cal BP) is distinguished palynologically by an increase in *Manilkara*-type and several other hardwood tree taxa which are only abundant in this zone (*Khaya*, *Carapa*-type

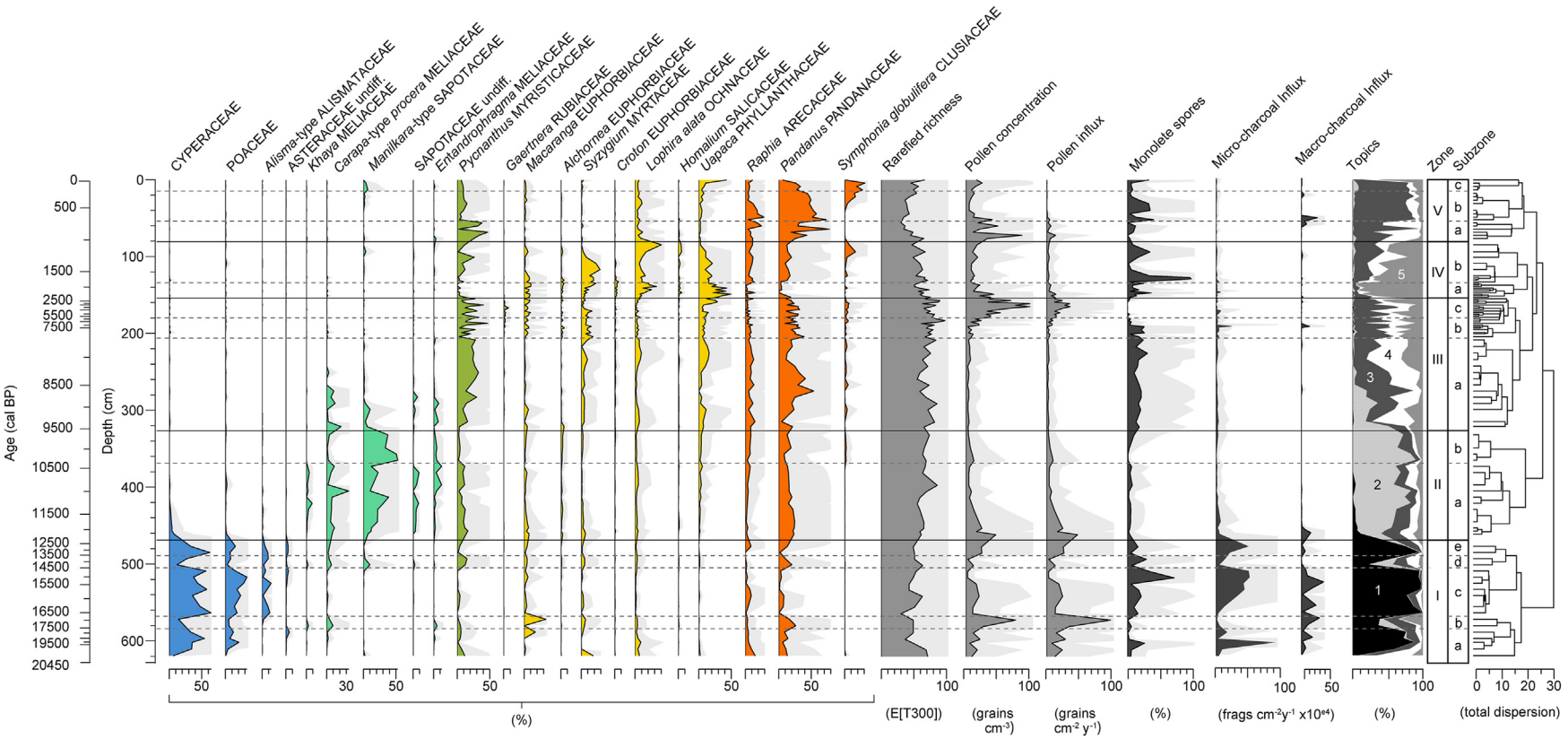

Fig. 5. CEN-17.4 pollen percentage diagram showing taxa >5% abundance and indicator taxa mentioned in the text (coloured by zone), plotted against depth (cm) and age (cal BP). The diagram is divided into five zones determined via CONISS analysis and fifteen subzones. Pollen concentration (grains cm^{-3}) and influx (grains cm^{-2} yr^{-1}) are also shown, along with rarefied palynological richness (E [T300], expected number of taxa in a count of 300 grains), monoloete spores (%) and charcoal influx rates (fragments cm^{-2} y^{-1} $x10^{e4}$). Correlated topic model community proportions (%) are also presented.

Table 1
Description of results.

Pollen zones *(Subzones)*	Depth (cm)	Age (cal BP)	Description
CEN-17.4_V	**81–0**	**1020–present**	**Stratigraphy:** Fibrous woody peat. Age-depth curve is steady and steep.
Vc	*15–0*	*200–present*	**Pollen:** Indicator taxa for this zone include the palm *Raphia* and two hardwood taxa, *Pandanus* and *Symphonia globulifera* (means 11.3, 41.3 and 7.0% respectively). *Pycnanthus* is abundant in the lower part of the zone and *Uapaca* is abundant in the uppermost sample, but most of the indicators of Zone II (*Syzygium*, *Lophira*, *Homalium*) are scarce. Pollen richness is lower than in Zone II.
Vb	*54–15*	*720–200*	**Charcoal:** Low influxes throughout (<75 fragments cm^{-2} yr^{-1}).
Va	*81–54*	*1020–720*	**Organic geochemistry:** The mean C/N ratio is 39.7, falling to 23.4 in the uppermost sample, reflecting an increase in total nitrogen. $\delta D_{n\text{-}C29\text{-}v\&icecorr}$ decreases to a minimum of −31.7‰ at 46 cm, then increases to −17.0‰ towards the top of the sequence.
			Inorganic geochemistry: In Subzone Va the concentrations of most elements fall substantially, recovering again in Subzone Vb. P and K are relatively more abundant here than elsewhere in the peats, and the uppermost sample shows a sharp peak in P, K, Mg, Mn, Cd and Zn.
CEN-17.4_IV	**154–81**	**2320–1020**	**Stratigraphy:** Fibrous woody peat. Age-depth curve is steady and steep.
IVb	*134–81*	*1730–1020*	**Pollen:** Indicator taxa include three abundant taxa, *Syzygium*, *Lophira* and *Uapaca* (means 12.3, 15.5, and 22.4% respectively), along with *Macaranga*, *Alchornea*, *Croton*, and *Homalium* in smaller proportions. All of these indicator taxa are hardwood trees. *Pycnanthus*, although present at up to 26%, is typically less abundant (mean 5.4%) than in the zone below. Subzone IVa is marked by peak values of *Uapaca* (up to 49.7%). In Subzone IVb the palynological assemblages become similar again to those in Zone III, with an increase in *Pycnanthus* and *Pandanus* at the expense of *Uapaca* (see NMDS biplot, Fig. 6). Palynological diversity remains high, though decreasing gradually upwards through the zone. Monolete pteridophyte spores are occasionally abundant, reaching their peak value of 100% (outside the main pollen sum) at 129 cm.
IVa	*154–134*	*2320–1730*	**Charcoal:** Low influxes through most of the zone, exceeding 120 fragments cm^{-2} yr^{-1} in only two samples (at 1710 and 1170 cal BP).
			Organic geochemistry: The mean C/N ratio is 47.3, similar to Zone III. δD_{C29} is above −20.7‰, less negative than in Zone III.
			Inorganic geochemistry: Similar to Zone III.
CEN-17.4_III	**327–154**	**9680–2320**	**Stratigraphy:** Fibrous woody peat. The age-depth curve is steep between 327 and 190 cm (Subzones IIIa and b) and much shallower between 190 and 154 cm (Subzone IIIc).
IIIc	*180–154*	*6200–2320*	**Pollen:** The *Manilkara*-type dominated assemblages of the zone below are rapidly replaced at the base of Zone III by a range of hardwood taxa. *Pycnanthus* (mean 19.2%) and *Gaertnera* (1.1%) are indicator taxa for this zone, although several other taxa (*Syzygium*, *Lophira*, *Uapaca*, *Raphia*, *Pandanus*) are also abundant. Palynological diversity is at its maximum in this zone. Monolete pteridophyte spores are abundant, especially in Subzones IIIa and IIIb.
IIIb	*206–180*	*7870–6200*	**Charcoal:** Low influxes through most of the zone, with the notable exception of a peak at 218 cm to ~134 fragments cm^{-2} y^{-1}.
IIIa	*327–206*	*9680–7870*	**Organic geochemistry:** In Subzone IIIa the mean C/N ratio is 47.8, mean $\delta^{13}C_{bulk}$ is −29.8‰ and $\delta D_{n\text{-}C29\text{-}v\&icecorr}$ values are in places very negative (mean −36.7‰ but reaching −48.2‰ at 274 cm). In Subzone IIIb C/N and $\delta^{13}C_{bulk}$ show little change, while $\delta D_{n\text{-}C29\text{-}v\&icecorr}$ values vary around a mean of −33.8‰. In Subzone IIIc there is a marked peak in C/N to an extremely high value of 82.3, accompanied by a well-marked minimum in $\delta^{13}C_{bulk}$ to −31.0‰, $\delta^{13}C_{n\text{-}C29}$ values remain invariant, a peak in $\delta^{15}N_{bulk}$ to 7.0‰, and a less distinct minimum in $\delta D_{n\text{-}C29\text{-}v\&icecorr}$ to −40‰.
			Inorganic geochemistry: Ca, Sr and Na increase substantially just above the base of the zone, at the expense of Fe, and remain proportionally important throughout the rest of the sequence.
CEN-17.4_II	**469–327**	**12,650–9680**	**Stratigraphy:** Well humified, possibly detrital peat with occasional leaves or seeds below c. 375 cm, grading into fibrous woody peat above. Age-depth curve is steep.
IIb	*369–327*	*10,450–9680*	**Pollen:** At the base of the zone Cyperaceae and Poaceae rapidly decline, replaced by a distinctive assemblage of tree taxa; indicator taxa for this zone include the numerically-dominant *Manilkara*-type (mean 25.2%) and, in smaller amounts, *Khaya*, *Carapa*-type *procera*, Sapotaceae undiff. and *Entandrophragma* (means 1.6, 8.2, 2.9 and 4.2% respectively). from >60% in the underlying zone to <20% at the base of this zone, while tree taxa expand to >70%. *Pycnanthus*, *Pandanus*, and to a smaller extent *Raphia* and *Uapaca* are also important in this zone. Palynological richness is higher than in Zone I and increases upwards through Zone II, with many tree taxa present in low abundances. Monolete pteridophyte spores are consistently less abundant than in Zone I.
IIa	*469–369*	*12,650–10,450*	**Charcoal:** Influxes are substantially lower than in the zone below, typically less than 50 fragments cm^{-2} yr^{-1}.
			Organic geochemistry: The mean C/N ratio is 42.6, similar to Zone 1, while $\delta^{13}C_{bulk}$ is markedly more negative (mean −29.6‰). $\delta D_{n\text{-}C29\text{-}v\&icecorr}$ values fluctuate around a mean of −24.7‰.
			Inorganic geochemistry: Concentrations of most inorganic elements decline gradually upwards through the zone (Mg, Cd and Zn are exceptions in showing no declining trend). In proportional terms, Fe and Mg become more important at the expense of Al.
CEN-17.4_I	**629–469**	**20,400–12,650**	**Stratigraphy:** Mottled light to very dark grey clayey silts below 599 cm (~19,600 cal BP), increasingly organic above 610 cm; peat (defined as LOI >65%) above 599 cm. The age-depth curve in the silts is not well constrained; the age-depth curve in the peats is less steep than in Zone II. The clayey silts have a mean particle size of 7.9 μm with no indication of a stratigraphic trend. The peats below c. 510 cm are very well humified, amorphous, with infrequent macrofossils, grading into slightly fibrous peat with occasional leaf fragments and seeds above.
Ie	*489–469*	*14,000–12,650*	**Pollen:** The indicator taxa for this zone are Cyperaceae (mean 37.6%), Poaceae (13.1%), *Alisma*-type (4.3%) and Asteraceae undiff. (1.5%). These four taxa typically covary (see topic model results), being most abundant in Subzones Ia, c, and e. Several other hardwood tree taxa are important, especially in Subzones Ib and d, including *Carapa*-type *procera*, *Manilkara*-type, *Pycnanthus*, *Macaranga*, *Syzygium*, *Lophira*, *Raphia* and *Pandanus*. Monolete pteridophyte spores are abundant.
Id	*505–489*	*14,850–14,000*	**Charcoal:** Microscopic charcoal is very abundant throughout this zone, especially in Subzones Ia, c and e, peaking at ~1420 fragments cm^{-2} yr^{-1} at 603 cm.
Ic	*568–505*	*17,550–14,850*	**Organic geochemistry:** The mean LOI value in the silts (below 599 cm) is 16.8%. $\delta^{15}N_{bulk}$ values in the silts are at a maximum for the sequence, peaking at 8.0‰. LOI in the peats reaches 90.4% at 597 cm and increases gradually throughout the remainder of the zone, interrupted by reversals (e.g. to 79.2% at 545 cm in Subzone Ic). $\delta^{15}N_{bulk}$ values are <2‰ in the peats. C/N values are low throughout the zone, with a mean of 39.3; peak values are
Ib	*584–568*	*18,200–17,550*	
Ia	*629–584*	*20,400–18,200*	

Table 1 (*continued*)

Pollen zones *(Subzones)*	Depth (cm)	Age (cal BP)	Description
			achieved in Subzones Ib and d. $\delta^{13}C_{bulk}$ values oscillate markedly around a mean of −24.8‰ with $\delta^{13}C_{n\text{-}C29}$ values around a mean of −32‰. $\delta D_{n\text{-}C29\text{-}v\&icecorr}$ values fluctuate around a mean of −21.1‰. **Inorganic geochemistry:** The clayey silts below 599 cm have a characteristic signature with high concentrations of Al accompanied by a suite of rarer elements (Pb, Cs, U, Rb, Li, V, Cu, Ag, Cr). These all become less abundant above 599 cm and throughout Subzone Ib, but almost all of them increase again in the middle of Subzone Ic, coinciding with the drop in LOI to 79.2%. There are slight differences in the signatures of these events (e.g. less Li and K, more Ni and As in Subzone Ic). In the peats above 599 cm, Al and Fe are proportionally the most important elements, Fe tending to increase proportionally at the expense of Al, with Ti and Mg also consistently abundant.

procera, Sapotaceae undiff. and *Entandrophragma*), accompanied by the other tree taxa found in Zone I. The chemistry of the peat is different (more negative $\delta^{13}C_{Bulk}$, higher C/N, proportionally less Al and more Fe) and less variable than in Zone I. These factors, along with the shape of the age-depth curve, suggest that peat accumulation rates increased during this period. Charcoal influxes drop to very low levels at the start of Zone II and remain low until Zone V.

Zones III (9680–2320 cal BP) sees a decline in *Manilkara*-type and an expansion of several taxa which remain important for the rest of the record. Zone III is characterised by *Pycnanthus* and (in the upper part) *Gaertnera*, but *Syzygium*, *Uapaca*, *Raphia*, and *Pandanus* are also important. The inorganic geochemistry of Zone III is marked by a large increase in the relative abundance of Ca and Na at the expense of Fe. The 'Ghost interval', the stratigraphic interval coinciding with a shallower gradient in the age-depth profile, starts just before the base of Subzone IIIc and ends at the base of Zone IV (i.e. between 190 cm/7520 cal BP and 151 cm/2150 cal BP). This peat representing this interval shows a sharp increase in C/N and minor changes in several other proxies (increased TC, decreased LOI and $\delta^{13}C_{Bulk}$); pollen concentration increases substantially, but there is little compositional shift in the pollen assemblages.

Zone IV (2320–1010 cal BP) sees an increase in the gradient of the age-depth profile and an inferred recovery of peat accumulation. C/N, TC, LOI and $\delta^{13}C_{Bulk}$ also revert to values similar to those in Subzone IIIa. There is a marked palynological change at the base of the zone towards assemblages dominated by *Lophira* and *Uapaca*, joined by *Syzygium* and *Symphonia globulifera* in Subzone IVb.

Zone V (1010 cal BP–present) sees a return to pollen assemblages very similar to those in Zone III, but with a greater abundance of *Pandanus* and, in the upper part, *Symphonia globulifera* and *Uapaca*. Isolated peaks in macrocharcoal (but not microcharcoal) occur, especially at the Subzone Va/b boundary. P and K concentrations both increase markedly towards the top of the sequence.

The NMDS analysis (Fig. 6) highlights an overall trend in the dataset with decreasing Axis 1 scores moving up-core. The NMDS analysis also emphasizes the overlap between assemblages in Zones III–V, and shows Zone IV as being moderately distinctive (positive Axis 2 scores). The CTM analysis provides a different, complementary perspective on the structure of the pollen data which may better reflect ecological realities (Fig. 7). It identifies five 'topics' (groups of covarying taxa) which may be interpretable as representing consistent species associations in the ecosystem (see discussion below). The first of these topics is characterised by Cyperaceae, Poaceae and *Alisma*-type, already noted as indicator

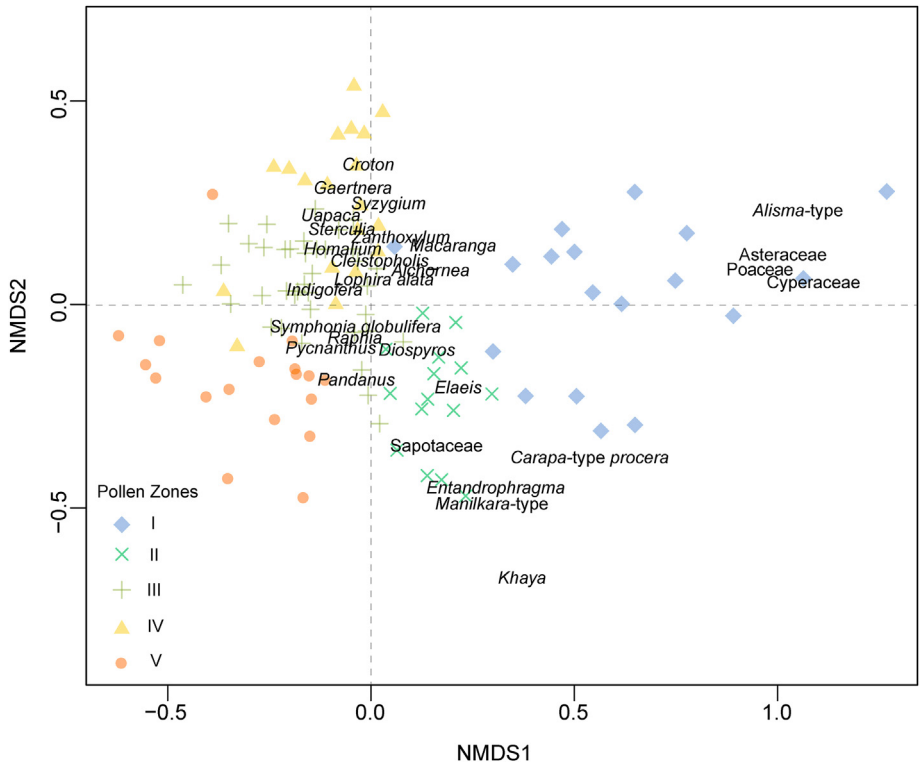

Fig. 6. Non-metric multidimensional scaling (NMDS) ordination of pollen data (>5% abundance). Symbols and colours represent the different pollen assemblage zones identified via CONISS analysis.

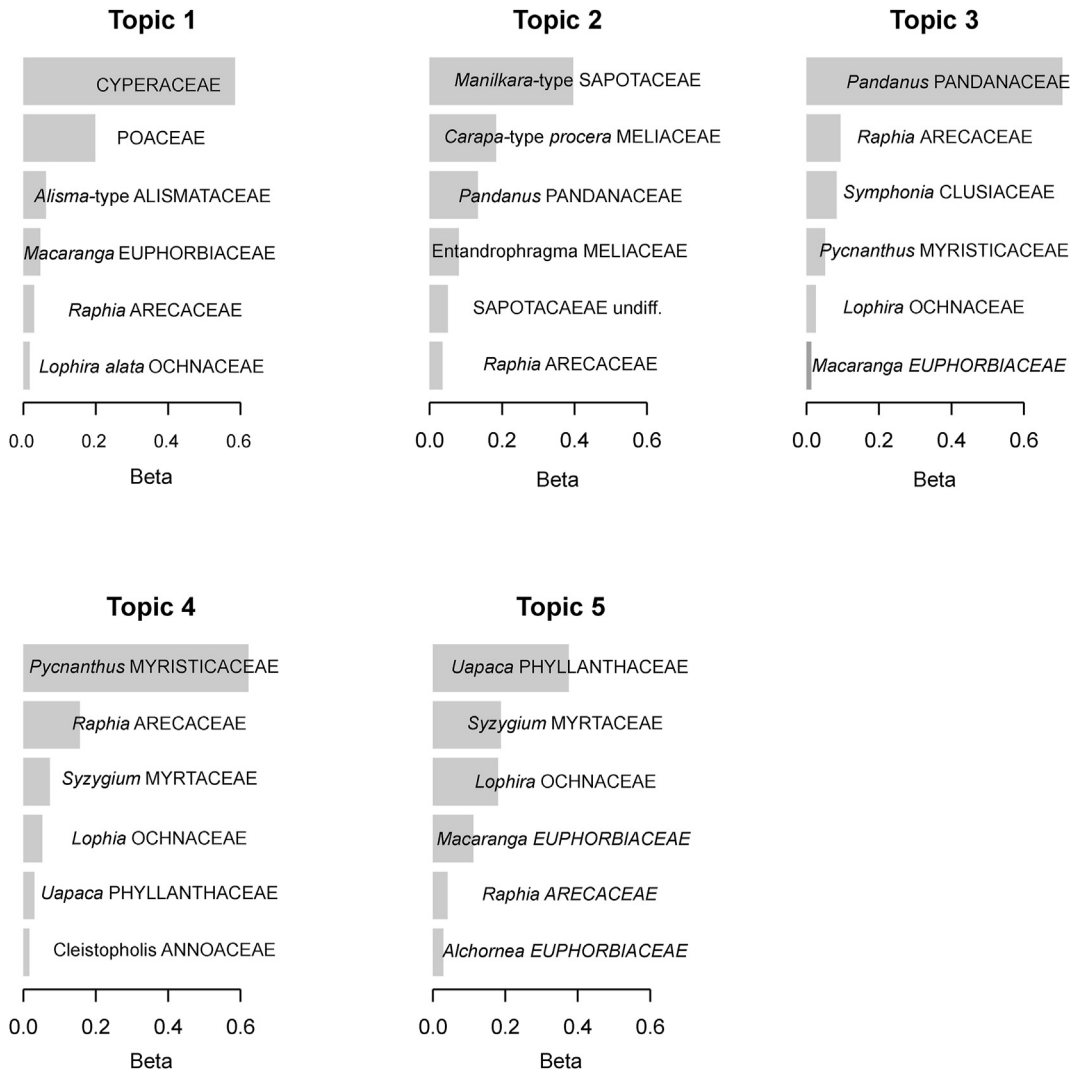

Fig. 7. Correlated topic model bar charts. Beta values show the relevant contribution of the dominant taxa to each topic model community.

taxa for Zone I. The second topic is dominated by *Manilkara*-type and *Carapa*-type *procera*, indicator taxa for Zone II, and the topic model indicates that *Pandanus* is consistently important alongside them. Topics 3–5 vary in abundance throughout Zones III to V: Zone III sees an early decline in Topic 2 (*Manilkara*-type, *Carapa*-type *procera*), followed by successive increases in Topic 3 (*Pandanus*, *Raphia*, *Symphonia globulifera*) and Topic 4 (*Pycnanthus*, *Raphia*, *Syzygium*). The early part of Zone IV sees a distinctive increase in Topic 5 (*Uapaca*, *Syzygium, Lophira*) before a gradual return to a mix of Topics 3 and 4 in the later part of Zone IV and Zone V.

5. Discussion

5.1. Peat initiation and peatland development

Our age model indicates that peat initiation began at the core site of CEN-17.4 sometime between 20,400 and 17,500 cal BP, close to the centre of what would at the time have been a large, shallow depression (~45 km across with 3–4 m of elevation change along our east–west transect line; Davenport et al., 2020). The present-day landscape has a gentle north–south slope – the Ubangui and Likouala-aux-Herbes rivers which bound the site to the east and west, both flow southwards, falling only ~15 m over ~275 km – but in the absence of peat thickness data along a north–south transect we cannot say whether the site was a shallow valley or a closed basin before the peatland developed. At the time of peat initiation, fine-grained mineral sediment was being delivered to the site, most likely by low-energy overbank flooding by sediment-laden waters. The resulting impermeable substrate would have helped to sustain the waterlogged conditions necessary for peat initiation. High concentrations of elements including Al and Ti (Fig. 9) suggest that these sediments were derived from highly weathered soils. Around ~19,600 cal BP (599 cm) the material crossed the 65% LOI threshold that we use to define 'peat', but the fact that LOI continues to increase slowly upwards, associated with a decline in the concentration of lithophilic elements including Al and Ti, suggests that the site was repeatedly flooded (seasonally or more episodically) until at least 10,450 cal BP (top of Subzone IIa, when LOI values first exceed 95%).

Whether peat initiation at the site of CEN-17.4 was driven by climatic change or some other factor, such as a geomorphological change (e.g. drainage blockage) or an autogenic process such as paludification, is unclear from our data. Dargie et al. (2017) suggested that peat initiation in the CCB might largely have been due to a shift to a wetter climate at the start of the Holocene, as the peat

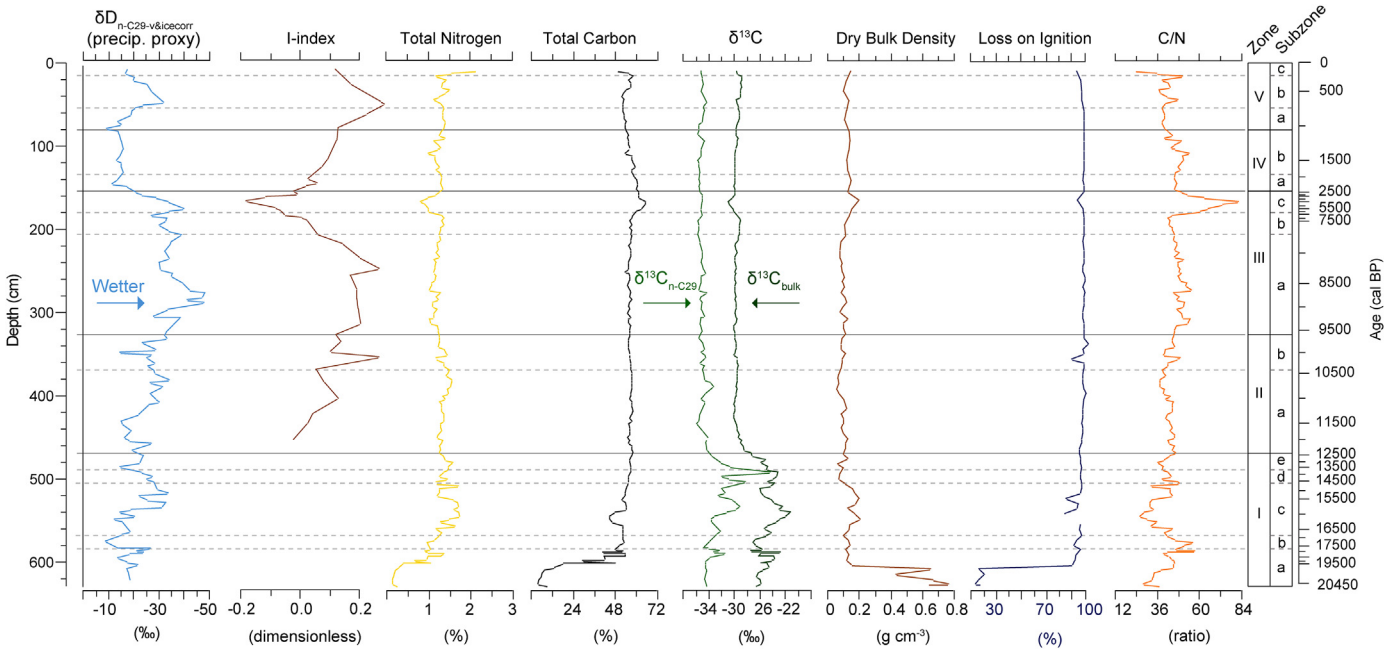

Fig. 8. Proxies of CEN-17.4 including the precipitation proxy ($\delta D_{n\text{-}C29\text{-}v\&icecorr}$ (‰), Garcin et al., 2022), I-index (Garcin et al., 2022), total carbon and nitrogen (%), $\delta^{13}C_{bulk}$ (‰) (right, dark green) and $\delta^{13}C_{n\text{-}C29}$ (‰) (left, light green, Garcin et al., 2022), dry bulk density (g cm^3), loss on ignition (%), and C/N ratio plotted against depth (cm) and age (cal BP). Pollen assemblage zones and subzones are also shown.

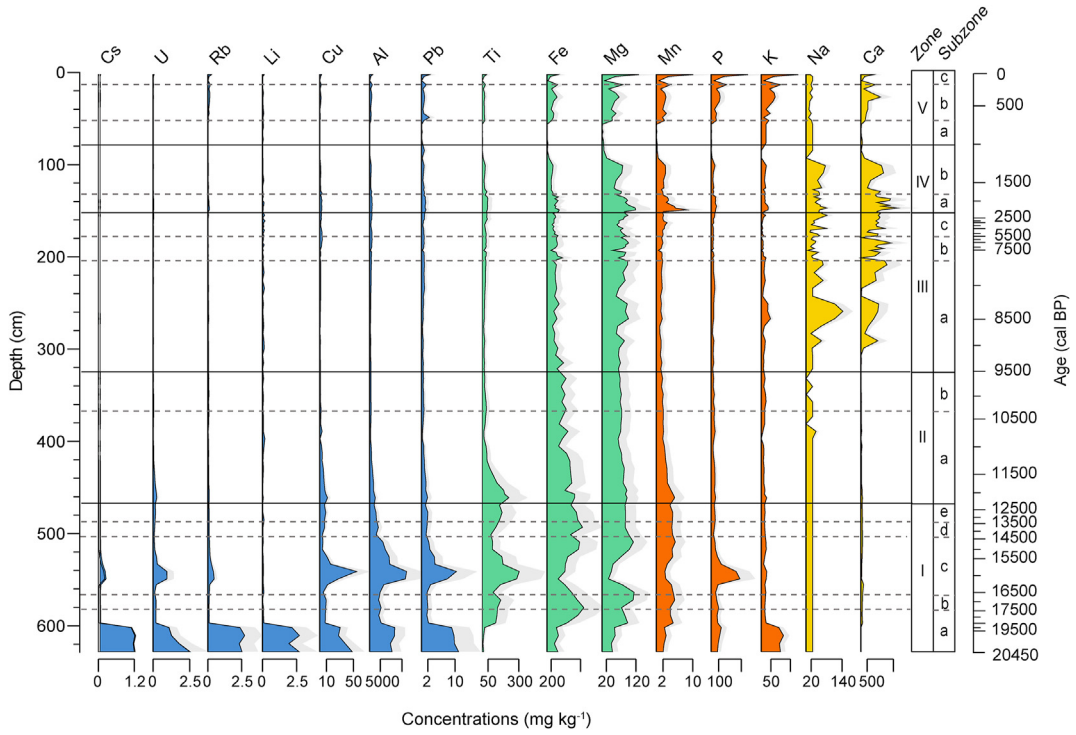

Fig. 9. ICP-MS record of CEN-17.4 showing selected element concentrations (mg kg^{-1}), coloured by dominance in each pollen assemblage zone (determined via indicator analysis), against depth (cm) and age (cal BP).

initiation dates then available were almost all from the early Holocene. The dating of CEN-17.4 demonstrates that peat was in fact accumulating long before the start of the Holocene, at least in places. Palaeoclimatic records from the region and climate modelling studies (Hamilton and Taylor, 1991; Schefuβ et al., 2005; Weijers et al., 2007; Liu et al., 2009; He et al., 2013) indicate that the climate of equatorial Africa between ~19,000 and ~17,000 cal BP was drier and cooler than today, with the driest/coldest conditions around the time of the deposition of Heinrich 1 (H1) in the north Atlantic, ~17,000–16,000 cal BP (e.g. Weijers et al., 2007; Bayon et al., 2012, cf. Andrews and Voelker, 2018). Temperatures began to increase gradually from ~17,000 and levelled off around 8000 cal

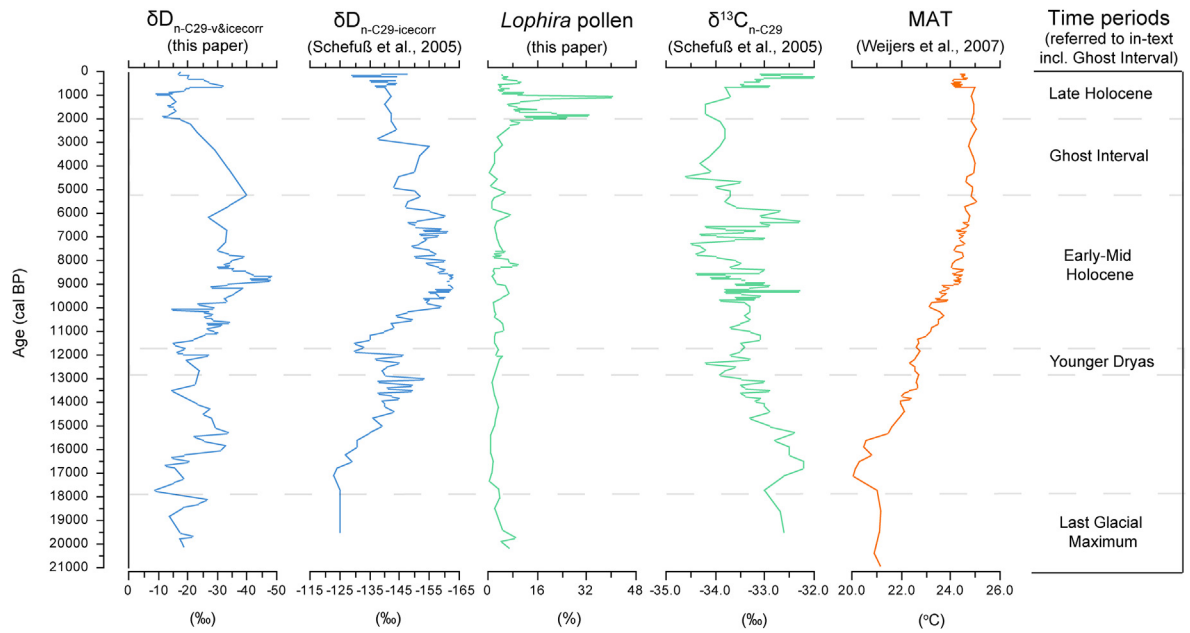

Fig. 10. Climate proxy data; $\delta D_{n\text{-}C29\text{-}v\&icecorr}$ (‰) (Garcin et al., 2022) from CEN-17.4 plotted with the $\delta D_{n\text{-}C29\text{-}icecorr}$ (‰) and $\delta^{13}C_{n\text{-}C29}$ (‰) record from Schefuß et al. (2005), mean annual temperature (MAT) reconstruction from Weijers et al. (2007), and the *Lophira* pollen curve from CEN-17.4, against depth (cm) and age (cal BP). Time periods referred to in the text are annotated, as well as the 'Ghost Interval' (period of reduced peat accumulation and increasing $\delta D_{n\text{-}C29\text{-}v\&icecorr}$ (‰) at CEN-17.4).

BP (Weijers et al., 2007). Precipitation is thought to have increased from ~17,000 cal BP until between ~12,500 and 11,500 cal BP, when a marked decline is reflected in $\delta D_{n\text{-}C29\text{-}icecorr}$ (Schefuß et al., 2005) and Al/K (Bayon et al., 2012) records from the Congo Fan. Outside the Congo Basin itself, evidence for low lake levels has been observed at the same time at several sites (Roberts et al., 1993; Gasse, 2000; Stager et al., 2002; Peck et al., 2004). Precipitation increased again at the start of the Holocene, with peak climatic wetness occurring in many records during the early to mid-Holocene (~10,000–6000 cal BP: Schefuß et al., 2005; Bayon et al., 2012; Shanahan et al., 2015; see discussion below and Fig. 10).

The $\delta D_{n\text{-}C29\text{-}v\&icecorr}$ data from CEN-17.4, the most direct line of evidence for palaeoprecipitation available for our site, is broadly consistent with these other records in indicating that the climate during the Pleistocene was generally much drier than during the early–mid Holocene. However, the data indicate a small, short-lived increase in inferred precipitation at ~19,750 cal BP (603 cm), just before peat initiation. The clayey substrate, the continued importance of river flooding (evidenced by mineral material in the peat and sediment), and the site's topographic location at a low point on the interfluve, would all have tended to favour water-logging at that time, so that even a slight increase in rainfall might have been sufficient to initiate peat formation. Low atmospheric CO_2 concentrations (Gasse, 2000) and low atmospheric water vapour (Bush and Philander, 1998) might be expected to have a negative effect on plant water use efficiency and hence litter production under a dry climate, but the pollen and $\delta^{13}C_{bulk}$ data from Zone I indicate that C_4 plants (which photosynthesize more efficiently than C_3 plants under low atmospheric CO_2) were the dominant contributors of litter to the peat.

By ~12,100 cal BP (459 cm), well over a metre of peat had accumulated (some may have subsequently been lost by decomposition) at the site of CEN-17.4. The age-depth curve then steepens, coincident with warmer and wetter climatic conditions evidenced by $\delta D_{n\text{-}C29\text{-}v\&icecorr}$ and $\delta D_{n\text{-}C29\text{-}icecorr}$ (Garcin et al. (2022); Schefuß et al., 2005), reconstructed MAT (Weijers et al., 2007), and sediment Al/K ratios (Bayon et al., 2012) and with an increase in lignin-rich C_3 vegetation (evidenced by the palynological evidence for replacement of herbs by trees, and the decrease in $\delta^{13}C_{bulk}$), suggesting rapid litter and hence peat accumulation until 190 cm (~7520 cal BP). At this point – the lower boundary of the 'Ghost Interval' of Garcin et al. (2022) – the age-depth curve flattens markedly, until 151 cm (~2000 cal BP). Garcin et al. (2022) argued, using the palaeoenvironmental proxies discussed here and additional data from two other sites in the CCB (Lokolama and Bondamba), that climatic drying from during the second half of the Holocene resulted in falling water tables, which led to contemporaneous and secondary decomposition of peat. The drying trend, marked in CEN-17.4 by a trend towards more positive $\delta D_{n\text{-}C29\text{-}v\&icecorr}$ values, began ~5000 cal BP and strengthened over time, culminating around 2000 cal BP. The trend in $\delta D_{n\text{-}C29\text{-}v\&icecorr}$ is accompanied by a decline (from ~30 to <5% by 2000 cal BP) in two of the most abundant swamp forest taxa, *Pandanus* and *Pycnanthus*, and by an increase in light-demanding and pioneer taxa, as water tables likely deepened. This change in forest structure and composition (discussed further below) involved a shift to taxa tolerant of the increasingly dry conditions. The I-index from Rock-Eval pyrolysis (Fig. 8) indicates intense decomposition of peat during this interval, associated with higher TOC values, indicating that the peat is dominantly composed of highly refractory organic matter (Garcin et al., 2022). The C/N ratio reaches a substantial peak at 164 cm, indicating preferential loss of nitrogen through aerobic decomposition of peats formed just before the driest interval. A similar peak in $\delta^{13}C_{bulk}$ likewise suggests preferential loss of labile organic matter. Garcin et al. (2022) estimate that up to 4 m of peat may have been lost to secondary decomposition during this interval.

Above 151 cm (~2000 cal BP) the gradient of the age-depth curve increases, suggesting that peat accumulation resumed. Hydrophilic swamp forest taxa (*Pandanus* and *Pycnanthus*) gradually recover, suggesting that soil moisture stabilized or increased, despite $\delta D_{n\text{-}C29\text{-}v\&icecorr}$ values remaining high and stable until ~900 cal BP. This may be due to a decrease in the strength of the dry season, which could result in higher water tables with no

detectable change in $\delta D_{n\text{-}C29\text{-}v\&icecorr}$ values.

Taken together, the evidence presented here from CEN-17.4, along with the independent palaeoclimatic data from the Congo Fan, suggests that climatic change has been important in controlling peat accumulation and decomposition in the Ekolongouma peatland. Late Glacial and early Holocene patterns of peat accumulation have yet to be studied at other peatlands within the CCB. However, the age-depth models from Lokolama and Bondamba presented by Garcin et al. (2022) suggest that a 'Ghost Interval' may be a widespread, perhaps ubiquitous feature of the CCB peatland stratigraphies, reflecting a severe drying event culminating around 2000 cal BP. This conclusion is consistent with a wide body of evidence from West and Central Africa which indicates increased aridity after ~4000 cal BP (Shanahan et al., 2015; Collins et al., 2017; Garcin et al., 2018). In particular, our record is relevant to understanding the Late Holocene Rainforest Crisis (LHRC), a widespread disturbance of rainforest vegetation between ~3000 and ~2000 cal BP identified at a number of locations in central Africa (Ngomanda et al., 2009; Maley et al., 2018). The exact timing, extent and causes of this event have been debated (Vincens et al., 1999; Giresse et al., 2020; Bayon et al., 2019; Garcin et al., 2018), but the evidence presented here and by Garcin et al. (2022) points to climatic drying being an important influence on the CCB peatlands at this time.

Despite the apparent substantial loss of peat represented by the 'Ghost Interval', the long-term net peat accumulation rate at CEN-17.4 is the highest recorded in the Ekolongouma peatland, with a value of 0.31 mm y^{-1}. This value is nonetheless at the low end of the ranges reported from domed peatlands elsewhere in the tropics (e.g. typically 0.54 mm y^{-1} in Central Kalimantan, 1.77 mm y^{-1} in Sumatra and 1.89 mm y^{-1} in East Kalimantan (Dommain et al., 2011); 1.27 mm y^{-1} at San Jorge (Kelly et al., 2017) and 1.88 mm y^{-1} at Aucayacu (Swindles et al., 2018), both in Peru; and 2.98 mm y^{-1} at San San Pond Sak, Panama (Phillips et al., 1997).

The spatial pattern of basal peat ages suggests that the nascent peatland in the Ekolongouma interfluve expanded laterally from the centre towards the margins sometime between ~19,600 and ~9500 cal BP (central estimates). The Pleistocene peatland at CEN-17.4 may have been part of a single continuous body of peat, or alternatively, just one of many small, separate peat bodies which occupied the deepest, wettest depressions in the interfluve. This pattern of peatland development is known from lowland tropical peatlands elsewhere, e.g. in Madre de Dios (Householder et al., 2012) and Quistococha (Kelly et al., 2020), Peru, where small pockets of peat formed in swales and pools, eventually infilling and coalescing over time to form the present day peatlands.

Long-term net peat accumulation rates decrease systematically in cores towards the margins of our site (Fig. 2), where peat thicknesses of 1.2–2.9 m are associated with basal peat ages of between ~9500 and ~10,500 cal BP. The lateral expansion of peat from the centre to the interfluvial margins may have been either a steady or an episodic process; the evidence currently available does not allow us to distinguish definitively between these possibilities given the large distances between dated cores, but the cluster of early Holocene dates suggests a burst of peat initiation at that time, perhaps related to wetter and warmer climates.

5.2. Interpreting the CEN-17.4 pollen record

Here we discuss our overall interpretation of this first pollen record from the CCB peatlands. The principles discussed here underpin the more detailed zone-by-zone palaeoenvironmental interpretations in Section 5.3.

Little is known specifically about the pollen source area and taphonomy of central African swamp forest taxa (Julier et al., 2021; Henga-Botsikabobe et al., 2020; Bengo et al., 2020), but many well-established principles can be assumed to apply to our record (e.g. Tauber, 1967; Prentice, 1985; Jackson and Lyford, 1999). The Zone I sediments and peats are likely to have a wider pollen source area than the peats in Zones II–V given the geochemical and sedimentological evidence for repeated flooding of the site by sediment-laden waters, and the dominance of herbs over trees at that time (evidenced by $\delta^{13}C_{bulk}$ as well as by the pollen data). The background presence of tree taxa in this zone may reflect pollen introduced in floodwaters rather than local production. As peat swamp forest became established, the pollen source area likely decreased as river flooding ceased and the forest canopy thickened, reducing wind speeds (Andersen, 1974; Whitney et al., 2019), and numerically important taxa in the pollen assemblages were likely to be growing at or very close to the sampling location. Some of our taxa are known to produce abundant pollen grains (e.g. *Uapaca, Alchornea, Macaranga* and *Celtis*; Lebamba et al., 2009; Tovar et al., 2019) and others not to (e.g. *Gilbertiodendron*: Tovar et al., 2019), but pollen productivity remains unknown for most taxa.

The integrity of the peat sequence as a palaeoenvironmental archive also needs to be considered critically. A key interval in CEN-17.4 in this respect is the 'Ghost Interval' between ~2000 and 7500 cal BP (151–190 cm). Pollen preservation is good throughout the interval, and the high pollen concentrations and steady pollen influx suggest that, as the peat matrix was mineralized away, the pollen was largely left intact. However, the peat sequence was greatly reduced stratigraphically and aerobic conditions may have facilitated bioturbation, mixing and disturbance of the remaining peat. Therefore, we interpret this part of the record with caution as it may not reflect a secure stratigraphic sequence.

Palynological taxa (i.e. identifiable morphotypes) may include pollen from plant species with very broad ecological tolerances, or several species with differing ecological tolerances, or species whose pollen has not yet been described in the literature. In many cases, the ecology of the plants themselves is not yet well understood. Accordingly, while we referred to local field data and to the ecological literature (particularly the African Plant Database v.3.4.0) for information on plant ecology, range and growth form, we used two complementary statistical analyses (NMDS and CTM) to explore the pollen record, to seek insights into the structures (e.g. species associations or successional patterns) that may exist in the vegetation that it represents.

The NMDS biplot (Fig. 6) maps the compositional dissimilarity between samples. Overall, there is a trend from right to left representing the overall trajectory of vegetation change over time, though with many reversals, particularly in Zones III to V. Samples in Zones I and II stand out as distinct from one another, while samples in Zones III to V overlap. This suggests that a key vegetational change reflected in the pollen dataset is the transition from Poaceae-Cyperaceae communities (Zone I), to communities dominated by trees typical of seasonally inundated forest (*Manilkara*-type, *Khaya*, *Carapa*-type *procera*: Zone II), to a mixed community of hardwood and more abundant monocot tree taxa (Zones III–V) which includes many of the taxa that are abundant in our census plots at the site today. Within that community there is differentiation between samples which are rich in hardwood swamp taxa such as *Uapaca* and *Gaertnera* (high NMDS axis 2 scores, especially in Zone II), and samples that are rich in the monocotyledons *Raphia* and *Pandanus*, along with *Pycnanthus* and *Symphonia globulifera* (low NMDS axis 1 and 2 scores, Zone V).

The CTM analysis identifies five 'topics' (Figs. 5 and 7), consistent co-occurrences of pollen taxa that may represent recurring ecological communities. This analysis suggests (in agreement with the NMDS) that the assemblages in Zones I and II represent distinct communities (Topic 1 [dominated by Cyperaceae and Poaceae] in Zone I, and Topic 2 [*Manilkara*-type and *Carapa*-type *procera*] in

Zone II). Within Zones III-V, the CTM suggests that there is some structure, but it is not as clearly defined as in Zones I and II: the topics are also not well defined, containing several overlapping taxa. Topics 3 and 4 represent a signal of hydrophilic swamp forest, oscillating between two dominant swamp forest taxa, *Pandanus* and *Pycnanthus,* with *Raphia* and *Symphonia globulifera* as accessory taxa in Topic 3; and *Raphia* (again), without *Pandanus* in Topic 4. Topic 5, dominated by the hardwood swamp trees *Uapaca* and *Syzygium* along with the light-demanding taxa *Lophira* and *Macaranga,* is most abundant in subzone IVa and b, following the 'Ghost Interval' and representing a drier and more disturbed forest association.

Taking both analyses into account, we conclude that during Zones III–V vegetational change at the site did not involve a succession of discrete communities but, rather, shifts in the relative abundance of taxa within a single community (i.e. a 'Gleasonian' scenario rather than a 'Clementsian' one: van der Valk, 1981; Burrows, 1990; Pickett et al., 2009). Compositional changes within Zones III and V may simply represent random interactions in the dispersal, recruitment, competition and mortality of individual taxa (Hubbell et al., 2001; Vellend, 2010). We interpret the expansion of Topic 5 in Zone IV as representing an environmentally-driven change associated with low precipitation, the changing composition reflecting an ecological response to a deeper water table and an increase in canopy openness. Once palaeo-precipitation increases (evidenced by a decline in $\delta D_{n\text{-}C29\text{-}v\&icecorr}$ values) the palynological assemblages are once more dominated by Topics 3 and 4, indicating hydrophilic swamp forest.

Observations of modern vegetation support these interpretations. Vegetation types that may be good analogues for Topics 1 (flooded grass/sedge fen), 2 (*Manilkara*-type dominated inundated swamp forest), and 5 (*Lophira*-dominated periodically inundated forest) are described by Moutsamboté (2012, discussed further below). A similar suite of taxa to those dominating Topics 3 (*Pandanus, Pycnanthus* and *Raphia*) and 4 (*Pycnanthus, Raphia,* and *Syzygium*) are observed in present-day vegetation plots along the CEN and EKG transects.

5.3. The palaeoenvironmental record at CEN-17.4

5.3.1. Zone I: 20,400–12,650 cal BP

The abundance of Cyperaceae, Poaceae and *Alisma*-type pollen in Zone I indicates an open, herbaceous and/or aquatic palaeoenvironment. The $\delta^{13}C_{Bulk}$ record confirms that the organic matter in Zone I is mostly derived from C_4 vegetation (i.e. grasses and sedges). Cyperaceae (e.g. *Cyperus difformis* L., *C. haspan* L.) and Poaceae (e.g. *Echinocloa stagnina* (Retz.) P. Beauv., *Vossia cuspidate* (Roxb.) Griff.) are frequently recorded in Congo Basin rivers and/or lakes, often forming floating mats (Bouillenne et al., 1955; Deuse, 1960; Hughes, 1992; Laraque et al., 1998; Moutsamboté, 2012). Elenga et al. (1991) record an 8 km-wide peatland, Bois de Bilanko in the Bateke Region, ROC, with a vegetation cover of *Syzygium* forest (*Syzygium* pollen is present in low abundance in Zone I at CEN-17.4) and floating mats of Poaceae and Cyperaceae. An alternative, but less likely analogue is a different kind of seasonally-inundated open savannah vegetation (including the grasses *Hyparrhenia diplandra* (Hack.) Stapf and *Setaria restioides* (Franch.) Stapf), presently found bordering the Likouala-aux-Herbes River, developing hydromorphic soils on recently deposited alluvium (Moutsamboté, 2012). These grasslands form part of a succession from savanna to seasonally-inundated forest dominated by *Lophira alata* Banks ex C. F. Gaertn. and *Daniella pynaertii* De Wild. (Moutsamboté, 2012).

Alisma-type pollen is recorded in Zone I. Moutsamboté (2012) records a community dominated by *Ranalisma humile* (Rich.) Hutch. (Alismataceae), which produces pollen of this type (Argue, 1974; Qing-feng et al., 1997), growing in shallow, calm, humic-rich muddy waters, near Mokole in the eastern DRC; a similar community is also frequently found in small tributaries of the Congo River, in the Yangambi region of the DRC (Léonard, 1996). *Ranalisma* is considered a pioneer aquatic genus, floating or submerged, which can colonize recently exposed substrates and shallow creeks. Alismataceae pollen was also found in sediments at Lac Tele, just north of our site (Laraque et al., 1998).

Throughout Zone I, especially in Subzones Ib and Id, numerous tree taxa are present in small amounts, including *Carapa*-type *procera, Manilkara*-type, *Pycnanthus*, *Macaranga*, *Raphia*, and *Pandanus*. High $\delta D_{n\text{-}C29\text{-}v\&icecorr}$ values in Subzones Ib and Id suggest that dry conditions during these intervals may have caused temporary reductions in flooding depth and/or frequency, allowing trees and shrubs to increase in abundance. *Carapa-type procera* and *Manilkara*-type can be abundant in flooded forests (see Zone II, below). The other taxa listed above are also found in open, wet environments, so it is likely that these trees were present, either in stands or as scattered individuals, close to the core site, or that their pollen was transported to the site from adjacent flooded forests. The present-day forest bordering the seasonally-inundated savanna of the Likouala-aux-Herbes is characterised by *Lophira alata* and other hydrophilic taxa including *Manilkara*-type, *Alchornea* and *Macaranga* (Moutsamboté, 2012), which occur in low abundance in Zone I. It is not unusual to find the pollen of late-successional swamp forest taxa in earlier successional phases, as later vegetation communities were likely to have been recruited from nearby assemblages (Morley, 1981). However, it is possible that some of the tree pollen in this zone was transported from further afield (cf. Section 5.2, above); *Macaranga* in particular is known to be well-dispersed with high pollen production (Laraque et al., 1998; Vincens et al., 2000, 2006), and the bisaccate pollen of *Podocarpus*, a montane genus, may be accounted for by long distance dispersal.

Oscillations in the pollen and $\delta D_{n\text{-}C29\text{-}v\&icecorr}$ records during Zone I highlighted by the subzonation may reflect climatic changes associated with intervening cool/dry and warm/wet periods between the base of our record (~20,400 cal BP) and 12,650 cal BP, reconstructed from Congo Fan sediments and other palaeoclimatic records (discussed in Section 5.1). However, the interaction between precipitation and evaporation (influenced by changes in temperature) and the changing influence of river flooding at the site make it difficult to predict the relationship between climate, local water tables, and peatland ecology during Zone I. Climatic changes were likely spatially variable, and notable differences exist between our CEN-17.4 $\delta D_{n\text{-}C29\text{-}v\&icecorr}$ record and the $\delta D_{n\text{-}C29\text{-}icecorr}$ record from core GeoB 6518–1 from the Congo Fan (Schefuβ et al., 2005), possibly because the latter incorporates a broader, basin-wide signal. Seasonality is also potentially important – a longer and/or more intense dry season can be more important to plants than a decline in total annual precipitation – but it is difficult to estimate seasonality reliably from the proxy records available.

The $\delta D_{n\text{-}C29\text{-}v\&icecorr}$ record at CEN-17.4, which we interpret as a proxy for the total amount of precipitation at the site following Garcin et al. (2022), indicates generally low precipitation in Zone I, consistent with existing reconstructions of a dry climate. Oscillations in this record indicate that the period ~16,000–14,000 cal BP (Subzone Ic) was relatively humid, compared to Subzones Ib (~18,200–17,550 cal BP) and Ie (~14,000–12,650 cal BP) which were generally drier. These oscillations do not correlate consistently with patterns in the pollen record or in other proxies such as dry bulk density or C:N ratio (Fig. 8). The final maxima in Poaceae and Cyperaceae coincide with low precipitation during the interval 14,000–11,450 cal BP (Subzones Ie and Iia – discussed further

below). There is evidence for episodic fluvial inundation (e.g. fluctuating LOI in Subzone Ic) at the core site during this interval which may reflect river channel migration, potentially another important influence on site development during Zone I.

The geographically closest Late Glacial palynological record to CEN-17.4 is Ngamakala Pond (Elenga et al., 1994, 2004), a wetland occupying a small basin on the Bateke Plateau (400 m a.s.l.), 550 km to the south. This record spans the past ~24,000 years and records a transition from "hydromorphous forest" (including Sapotaceae undiff. and *Syzygium*) to "hydrophytic grassland" (including *Xyris* and *Nymphaea lotus* L.) between ~24,000 and ~13,000 cal BP, attributed to an inferred decrease in precipitation and increased seasonality. The Late Glacial vegetation histories are broadly similar, with both sites being dominated by open sedge/grassland, but in detail the palynological assemblages at the two sites differ markedly, with CEN-17.4 being dominated by Cyperaceae, Poaceae and *Alisma*-type, versus *Xyris* and *Nymphaea lotus* at Ngamakala, possibly reflecting individual site characteristics (e.g. soil or water chemistry).

Another pollen record from the southern ROC, Bilanko, also spans this period; though poorly dated, it shows abundant montane taxa (*Ilex*, *Olea* and *Podocarpus*) prior to 11,000 kyr BP. Barombi Mbo (Cameroon) likewise shows abundant *Olea*. The migration of montane taxa to lower altitudes during the LGM has been related to an increase in trade-winds, which caused strong marine upwellings and productivity, and a fall in sea surface temperatures (SST) (Jansen et al., 1984; Mix and Morey, 1996). Lower SST may have increased the formation of low stratiform clouds, promoting the survival of montane taxa at lower altitudes than present (Maley and Elenga, 1993; Maley, 1996). Several authors (e.g. Colyn et al., 1991; Jahns, 1996; Maley, 1996) have raised the possibility that rainforest taxa may also have survived the driest conditions of the last glacial on floodplains in the CCB. At CEN-17.4, the dominance of Poaceae and Cyperaceae throughout the Pleistocene part of the record indicates that the site itself was not forested, but the persistent presence of several tree taxa discussed above indicates their presence somewhere within the pollen catchment of the site.

Charcoal influx rates are high throughout Zone I, especially in Subzones Ia, c and e, indicating that fire was an important process. Today, the Congo Basin is one of the most lightning-prone regions on Earth (Christian et al., 2003) and it is quite plausible that natural fires could take hold in dry grass-sedge vegetation during the dry season(s). Anthropogenic fire ignitions cannot be excluded, however, especially given that the open Pleistocene landscape is likely to have been easier to access than today's dense swamp forest. The fires are strongly associated with Topic 1, characterised by Cyperaceae and Poaceae, suggesting that fuel type may have been important in determining the fire regime, although fuel load and moisture typically also play a role in fire ignitions (McLauchlan et al., 2020). Fire is thought to be important in maintaining open savannah ecosystems where climatic and soil conditions would be sufficient to support forest cover, and fire may have played a role in delaying succession to swamp forest at CEN-17.4 (Veenendaal et al., 2018; Aleman et al., 2019).

5.3.2. Zone II: 12,650–9680 cal BP

The very top of Subzone Ie and the lower part of Subzone IIa (422–464 cm) show some evidence for reduced precipitation in the $\delta D_{n\text{-}C29\text{-}v\&icecorr}$ values, which are generally higher than in the previous subzones. The dry conditions ~12,000 cal BP are not associated with peat decomposition at this point in the record, likely due to the dominance of C4 vegetation, evidenced in the $\delta^{13}C_{n\text{-}c29}$ record (Fig. 8). The peat was also shallower here than during the Ghost Interval, with likely less surface water lost via overland flow, lessening the impact of any drying (Garcin et al., 2022). Proxy records from Lake Barombi Mbo in Cameroon (Giresse et al., 1994; Maley and Brenac, 1998), Lake Bosumtwi in Ghana (Shanahan et al., 2015) and Ngamakala Pond in ROC (Jansen et al., 1995) also indicate increased aridity at this time (Weijers et al., 2007; Schefuβ et al., 2005). However, the CEN-17.4 data show high sample-to-sample variability, particularly ~12,000 cal BP, similar to the $\delta D_{n\text{-}C29\text{-}icecorr}$ record from core GeoB6518-1 from the offshore Congo fan (Fig. 10; Schefuβ et al., 2005). Renssen et al. (2018), modelling global hydroclimate, suggest that the Congo Basin may have seen (at most) only small decreases in temperature (<1 °C) and soil moisture in response to perturbation of the global climate system between 12,900 and 11,700 cal BP, related to deglaciation and the drainage of Lake Agassiz, among other forcings. This finding is consistent with the CEN-17.4 $\delta D_{n\text{-}C29\text{-}v\&icecorr}$ data, which suggest some impact of regional- or global-scale perturbations to the climate system, but substantial modulation and modification of the signal by other factors.

By contrast with the $\delta D_{n\text{-}C29\text{-}v\&icecorr}$ data, the pollen data from CEN-17.4 spanning the Zone I and II boundary indicate a marked reorganisation of the ecosystem from a sedge-grassland with few trees, to a closed-canopy forest dominated by taxa typically found today in seasonally-inundated forests. The inferred decline in sedges and grasses at the site is supported by the $\delta^{13}C_{Bulk}$ record which shows an initially abrupt decrease around ~12,600 cal BP indicating a shift from C_4- to C_3-dominated vegetation, a transition that was fully completed by the start of the Holocene. This is consistent with the $\delta^{13}C_{n\text{-}c29}$ values which show a shift from high to low values ~12,000 cal BP reflecting the shift from a grass-to tree-dominated environment. Indicator taxa characterising Zone II include *Manilkara*-type, *Carapa*-type *procera, Khaya*, Sapotaceae undiff. and *Entandrophragma*. This assemblage, representing a seasonally-inundated forest community, is distinctive, separated clearly in the NMDS biplot and well defined by the topic model analysis (Topic 2). Other swamp forest taxa (notably *Raphia*, *Pycnanthus, Pandanus,* and *Uapaca*), which are present from the beginning of the record, remain consistently present in small amounts. The rarefied richness curve (Fig. 5) suggests that the diversity of the vegetation increased. Adjanohoun et al. (1988) and Moutsamboté (2012) describe a potential analogue for the Zone II environment in north-eastern ROC, south of Souanke, where the forest is dominated by *Manilkara*-type, *Entandrophragma, Carapa*-type *procera, Uapaca, Macaranga*, and *Pycnanthus*, with standing water. Campbell (2005) summarises earlier vegetation classifications (Lebrun and Gilbert, 1954; Evrard, 1968; Fay et al., 1989) indicating that all these taxa (except *Carapa*-type *procera* and *Pycnanthus*) are dominant in near-permanently inundated swamp forest. Therefore, the inference of a closed canopy, waterlogged, swamp forest environment for the vegetation in Zone II is well supported by the ecological literature.

It may be no coincidence that the major shift in vegetation defining the Zone I/II boundary took place during a climatically-driven reduction in precipitation, which may have allowed trees to become established at the site, outcompeting herbaceous vegetation. On the other hand, autogenic succession related to the gradual accumulation of peat (more than a metre by this point) could achieve the same effect, and certainly once the flooded forest community was in place, it persisted without interruption well into the Holocene, through the warming of climatic conditions and a precipitation increase indicated in the CEN-17.4 $\delta D_{n\text{-}C29\text{-}v\&icecorr}$ record from ~11,450 cal BP.

As peat continued to accumulate throughout the time of Zone II, there was a gradual reduction in the importance of river flooding

over time, evidenced by high LOI and reduced concentrations of lithophilic elements (notably Al and Ti). This decrease in allogenic input, accompanied by distinct shifts in vegetation composition (e.g. Zones II–III), suggests that a fen–bog transition was underway, as the peatland became progressively more ombrotrophic (Hughes, 2000; Hughes and Barber, 2004; Lähteenoja et al., 2009; Kelly et al., 2017). At CEN-17.4 this appears to have been a gradual process. The decline in inputs of mineral material may have been driven not just by the upward accumulation of peat but also by the lateral expansion of the peatland towards the adjacent rivers, which would act to limit the ingress of floodwater and reduce its velocity and therefore sediment load (cf. Mertes, 1997).

The near-total absence of micro- and macrocharcoal in Zone II (and most of the remainder of the record) suggests that fire had ceased to be important. It is possible that, beneath the swamp forest canopy, the litter did not become seasonally dry, so natural fires could not take hold. Alternatively, whereas deliberately burning the dense grass/sedge vegetation in the late Pleistocene (Zone I) may have been useful for hunting, the anthropogenic use of fire in the Holocene flooded forest (Zone II) may have been less practical and/or advantageous; to our knowledge, burning is not carried out in the swamp forest today.

5.4. Zone III: 9680–2320 cal BP

In Zone III, mixed swamp forest replaced the *Manilkara*-type forest of Zone II. The CEN-17.4 $\delta D_{n\text{-}C29\text{-}v\&icecorr}$ record indicates an increase in precipitation from the start of the Holocene to a peak between 8000 and 9000 cal BP. This peak is paralleled in other palaeoclimatic records from central Africa, which indicate high precipitation, high humidity and a reconstructed annual mean air temperature (MAT) in the Congo Basin of ~24–25 °C (e.g. Schefuβ et al., 2005; Weijers et al., 2007; Bayon et al., 2012; Shanahan et al., 2015). The CEN-17.4 pollen record indicates that the flooded forest of Zone II was gradually replaced during Zone III by a mixed swamp forest, largely lacking *Manilkara*-type and the other indicator taxa for Zone II, and dominated instead by taxa including *Pycnanthus*, *Gaertnera*, *Syzygium*, *Lophira, Uapaca*, *Raphia* and *Pandanus*, all of which have been recorded in census plots on the peatland today. Palynological richness is at its maximum, suggesting that the forest had become more diverse over time, which may simply represent an autogenic process driven by gradual immigration and establishment of additional taxa, rather than any environmental driver (cf. MacArthur and Wilson, 1967).

While peat appears to have been accumulating steadily in Subzone IIIa, in Subzones IIIb and IIIc the age-depth curve flattens (the 'Ghost Interval', i.e. 151–190 cm/2150–7520 cal BP, Section 5.1 above). The near-total loss of several metres of peat means that the stratigraphic integrity of this part of the record is doubtful. Although pollen concentrations are very high, especially in Subzone IIIc (suggesting that the pollen remained intact as the peat mineralized), and there is substantial sample-to-sample variation in the pollen taxa, overall, we infer that there was little compositional shift in the vegetation during the period represented by the 'Ghost Interval' until ~2000 cal BP, in Zone IV (discussed below).

The dominant taxa in the pollen assemblages in Zone III – those that characterise Topics 3 and 4 – are all abundant in census plots at the site today (indeed they become important again in Zone V, in the uppermost part of the sequence). The modern vegetation is diverse and spatially variable; some of the variation may relate to the large-scale structure of the peatland (e.g. the increasing abundance of *Raphia* towards the centre of the peatland), but much of the variation is not easily explainable. The pollen data suggest that, throughout the 7000 years covered by Zone III, the vegetation composition at the location of CEN-17.4 fluctuated around a mean, possibly simply as a result of random vegetation dynamics. Besides the gradual decline of Topic 2 taxa (*Manilkara*-type, *Carapa*-type *procera*) across the Zone II/III transition, there is little evidence for directional, successional change in Zone III, suggesting that the peatland vegetation may have achieved something close to a state of dynamic equilibrium.

5.4.1. Zone IV: 2320–1010 cal BP

This zone includes the end of the 'Ghost Interval', ~2000 cal BP, when there was a significant decline in several swamp forest taxa including *Raphia*, *Pandanus* and *Pycnanthus*, and an increase in pioneer and light-demanding taxa including *Lophira*, *Alchornea,* and *Macaranga* (Laraque et al., 1998; Brncic et al., 2007; Kiahtipes et al., 2011). Other indicator taxa for this zone include *Syzygium* and *Uapaca*, with *Croton* and *Homalium* in smaller proportions; Topic 5 (*Uapaca*, *Syzygium*, *Lophira*, *Macaranga*) becomes dominant, especially in Subzone IVa. Despite the increase in pioneers and light demanders, there is little expansion of grasses, sedges or herbs, which peak at just 2% at ~2000 cal BP, the point of lowest precipitation as inferred from the $\delta D_{n\text{-}C29\text{-}v\&icecorr}$ record, which suggests that the forest canopy remained largely intact. Rarefied richness declines markedly throughout this zone, suggesting the forest became less diverse (Fig. 5).

The shift in Zone IV (particularly ~2000 cal BP) to more heliophilic and drought-tolerant vegetation is consistent with a well-documented period of vegetation change in central Africa between 2500 and 2000 cal BP, the Late Holocene Rainforest Crisis (Giresse et al., 2020; Bayon et al., 2019; Maley et al., 2018; Garcin et al., 2018). Palaeoenvironmental records from Nyabessam swamp in south-western Cameroon (Ngomanda et al., 2009), Lakes Barombi Mbo (Maley and Brenac, 1998) and Ossa (Reynaud-Farrera et al., 1996) in southern Cameroon, Lakes Kitina (Elenga et al., 1996) and Nguene (Giresse et al., 2009) in Gabon, the Mopo Bai swamp in north-western ROC (Brncic et al., 2009) and Ngamakala Pond in south-western ROC, Elenga et al., 1994), all within the Greater Congo Basin, consistently show a shift to pioneer and grassland taxa and a decline in mature swamp forest taxa at this time (Maley et al., 2018), though there are variations in the nature and timing of the ecological changes. At Goualougo Lake, 200 km northwest of CEN-17.4, Brncic et al. (2007) record an increase in herbs, shrubs and light-demanding trees (especially *Lophira alata*) at ~2000 cal BP and independent evidence for drought from ~2800 to 2000 cal BP (an increase in dust proxies in the geochemical record). A record from marshland adjacent to the Bodingue River in the Ngotto forest of the Central African Republic, 300 km northeast of CEN-17.4 (Kiahtipes et al., 2011), shows an increase in pioneer taxa (*Triplochiton*) and oil palm (*Elaeis*) around 2000 cal BP, followed by an expansion of light-demanding taxa (Asteraceae, Cyperaceae and *Pycnanthus*) by ~800 cal BP; though poorly constrained, the chronology also shows a pronounced reduction in sedimentation rate after ~2000 cal BP, which Kiahtipes et al. attributed to reduced precipitation.

The cause of the Late Holocene Rainforest Crisis has been widely debated: it may have been driven by climatic drying, anthropogenic clearance, or a combination of the two (e.g. Maley et al., 2018; Garcin et al., 2018; Bayon et al., 2019; Giresse et al., 2020). The absence of compelling evidence for anthropogenic activity such as crop production or burning in the CEN-17.4 record suggests at most a minor, if any role for human impacts at our study site.

Subzone IVa sees a small increase (<1%) in *Elaeis guineensis* (oil palm) pollen. *Elaeis* has long been cultivated by Bantu populations and is sometimes considered to be an anthropogenic indicator in pollen diagrams (e.g. Sowunmi, 1999; Maley, 1987; Brncic et al., 2009; Bostoen et al., 2013), but it also grows wild in peatland forests today (e.g. Maley and Chepstow-Lusty, 2001; Kahlheber et al.,

2014, and authors' personal observation); other palaeoecological studies have also suggested that it is not a consistent indicator of human activity. For example, Brncic et al. (2007) noted a low abundance of *Elaeis* pollen from ~3300 cal BP at Goualougo Lake, but concluded that fluctuations in its abundance were more likely to have been driven by climate than by anthropogenic activity, as its abundance was correlated with dry climatic intervals. Several studies (Maley, 1999; Maley and Chepstow-Lusty, 2001; Maley et al., 2018; Maley et al., 2018, 2018) have concluded that the expansion of *Elaeis* following the forest fragmentation at ~2500 cal BP reflects its status as a natural pioneer, preceding the re-establishment of a mature forest, rather than related to anthropogenic activity. The limited expansion of *Elaeis* in the CEN-17.4 record during Subzone IVa therefore does not necessarily imply any human activity. There is likewise no evidence in the charcoal record for burning at the site at this time. There is thus no strong evidence that humans had a substantial impact this far into the peatland, almost 20 km from the nearest river.

In Subzone IVb swamp forest taxa re-expand, initially led by the heliophiles *Pandanus* and *Raphia*, despite $\delta D_{n\text{-}C29\text{-}v\&icecorr}$ values remaining high and stable indicating continued low precipitation and/or increased seasonality. *Lophira* remains a substantial component of the forest structure here, and has been seen to expand at numerous sites across the region around this time, with some variation in timing (Brncic et al., 2007, 2009; Ngomanda et al., 2009; Maley et al., 2018; Giresse et al., 2020). A mature swamp forest eventually became re-established, with a composition similar to that prior to the 'Ghost Interval' (i.e. in Zone III) but associated with markedly lower precipitation (more positive $\delta D_{n\text{-}C29\text{-}v\&icecorr}$). Thus, some recovery of the ecosystem appears to have occurred once the new precipitation regime stabilized. Recovery of forests following the LHRC is seen in other palaeoecological records from the region. For example, following a forest contraction at Ngamakala Pond ~3000 cal BP, the forest expanded again, persisting to the present day (Elenga et al., 1994). Small increases in rainfall (e.g. ~2300–2110 cal BP and ~1880–1345 cal BP) at Mopo Bai in the north-western ROC were accompanied by a rapid expansion of hydrophilic and shade-tolerant taxa (Brncic et al., 2009), suggesting that the vegetation responded rapidly to increasing precipitation. In addition to the forest recovery, the resumption of peat accumulation at CEN-17.4 after ~2000 cal BP is also in line with other records from across the Basin (Garcin et al., 2022; Elenga, 1992; Elenga et al., 1994). For example, in the Lope National Park, Gabon, Bremond et al. (2021) record that most peaty marshes established between 2150 and 1950 cal BP.

The detailed reconstruction of the 'Ghost Interval' in the CEN-17.4 record thus contributes to the growing body of evidence for a substantial climatic change with widespread and profound ecological consequences in Central Africa beginning ~5000 cal BP and peaking ~2000 cal BP. In particular, our record indicates that the LHRC was not restricted to terre firme rainforests, but also had a substantial impact on peatland carbon storage and on the composition of peatland vegetation. Maley et al. (2018) proposed that the floodplains of the CCB may have provided refugia for rainforest taxa, a suggestion supported by our pollen evidence for continued presence of forest throughout the Holocene, albeit with substantial turnover in community composition.

5.4.2. Zone V: 1010 cal BP – present

Overall, the data for Zone V indicate a similar environment to the pre-'Ghost Interval' swamp forest of Zone III. The key pollen indicator taxa for Zone IV/Topic 5 become scarce, replaced by Topics 3 and 4 (*Pycnanthus*, *Raphia* and *Pandanus*). We therefore interpret this zone as indicating that the swamp forest had largely recovered from the climatic event that created the 'Ghost Interval'. In detail, however, there are some important ways in which the ecosystem continued to change during Zone V.

Subzone Va continues the recovery initiated in the previous subzone and the assemblages here become very similar to those of Zone III, with abundant (but variable) *Pycnanthus*. Although microcharcoal influx is usually very low throughout Zone V, at the Subzone Va/b boundary there is a moderate peak in microcharcoal. The fact that this peak occurs during a transition to wetter climatic conditions does not rule out the possibility that this is a chance, natural, local phenomenon, but equally we cannot exclude the possibility of small-scale, local anthropogenic burning (the continuing low influx of microcharcoal is evidence against widespread burning).

Towards the top of Subzone Va and into Subzone Vb both *Raphia* and *Pandanus* become more abundant, followed a little later by *Symphonia globulifera*. Arguably, the expansion of these taxa can be interpreted as the continuation of a longer-term trend: all three taxa show a tendency towards greater abundance moving up through the core from Zone III onwards, albeit with numerous reversals. Inspection of the NMDS biplot (Fig. 6) confirms that, ignoring the disturbance associated with the 'Ghost Interval' in Zone IVa, the pollen assemblages show a steady compositional trend towards more negative Axis 1 scores across Zones II, III and V. This suggests that there may be a weak successional trend, spanning the last ~12,000 years, underlying substantial superimposed higher-frequency variation in vegetation composition (presumably driven partly by climatic change and partly by stochastic ecological processes such as competition). It is not clear whether this temporal trend bears a functional relationship to the present-day spatial vegetation patterning at the site (*Raphia* being more common towards the centre than the margins of the site; cf. e.g. Anderson and Muller, 1975; Phillips et al., 1991). Further research is needed to understand the drivers of present-day vegetation gradients and to test whether a similar long-term increase in *Raphia, Pandanus* and *Symphonia globulifera* occurs in other sequences from Ekolongouma and at other sites in the CCB.

On a finer temporal scale, variations in the pollen assemblages within Zone V may be partly attributable to climate change. Values of $\delta D_{n\text{-}C29\text{-}v\&icecorr}$ decrease throughout Subzone Va (indicating increasing precipitation), reach a minimum (i.e. wet conditions) in Subzone Vb between 300 and 600 cal BP, and then increase again (drying) into Subzone Vc at the top of the sequence. Several records from central Africa show similar evidence for climate variability during the last millennium, although the timing of inferred changes is not always the same, possibly reflecting the limitations of age-depth models rather than indicating regional variation in climate histories. For example, at Ngamakala Pond, Elenga et al. (1996) record a decline in heliophilic tree species such as *Pandanus* and Poaceae from ~490 cal BP, interpreted as indicating a return to wetter conditions. At Mopo Bai, Brncic et al. (2007) record an increase in moisture between 600 and 100 cal BP accompanied by the expansion of hydrophilic taxa such as *Pycnanthus*. At Lake Sinnda, Niari Valley, southern ROC (Vincens et al., 1994), Poaceae declines ~650 cal BP. Several proxies in the record from Kivesso, a coastal swamp near Diosso, southwest ROC, show a clear increase in precipitation from ~500 cal BP until ~300 cal BP (Malounguila-Nganga et al., 2017). Thus, the CEN-17.4 $\delta D_{n\text{-}C29\text{-}v\&icecorr}$ record adds to a regional body of data suggesting that the climate was wetter than today around 500 years ago. These climatic changes may have influenced vegetation changes – for example, peak abundance of *Pandanus* and *Raphia* coincides very approximately with the $\delta D_{n\text{-}C29\text{-}v\&icecorr}$ minimum – although there is no simple relationship between the isotope record and the pollen composition.

The uppermost sample is similar in composition to samples from Zone IV (the 'Ghost Interval'), plotting in a similar position in

the NMDS biplot, unlike the other samples in Zone V. The present-day vegetation surrounding the coring site includes *Uapaca mole, Raphia laurentii, Carapa procera, Xylopia aethiopica* and *Pandanus candelabrum* P. Beauv. *Uapaca* and *Pandanus* are well represented in the uppermost pollen sample, while *Raphia, Carapa-type procera* and *Xylopia* are also present but less abundant, probably reflecting variations in pollen production between species. While taphonomic effects should not be ruled out, replication in other cores and sites could shed light on the extent to which CCB peatland ecosystems have changed in recent decades. Our data suggest that, throughout its history, the ecosystem at the site of CEN-17.4 has rarely been static for long, which suggests that we should expect the present-day peatlands to be variable in time and space.

6. Conclusions

6.1. Timing and pattern of peat accumulation

This detailed multi-proxy study has explored the genesis and development of an interfluvial peatland in the central Congo Basin. Our age model indicates that peat began to accumulate some time between 20,400 and 17,500 cal BP on a clay-silt substrate, at the lowest point measured along the transect between the Ubangui and Likouala aux Herbes rivers, close to the centre of the peatland. Basal dates from four other cores at the site indicate that the peatland was much smaller during the Pleistocene than it is today, and that it expanded rapidly laterally during the early Holocene. Net long-term apparent peat accumulation rates decrease from the centre towards the peatland margins. Vertical peat accumulation at the peatland centre (CEN-17.4) was likely slow during the Pleistocene, then more rapid during the early Holocene. A drying interval, peaking ~2000 cal BP, caused the near-complete mineralization of several metres of pre-existing peat. Less well-constrained age-depth models from three other cores from Ekolongouma (and from two other sites in the CCB, Lokolama and Bondamba: Garcin et al., 2022), all show a similar age-depth pattern in the mid-Holocene. The driest period at the end of the decomposition interval identified at CEN-17.4 is coincident with an arid phase, the LHRC, seen across central Africa and often represented by a vegetation change between 3000 and 2000 cal BP. All four dated cores from Ekolongouma indicate that peat accumulation resumed after ~2000 cal BP.

6.2. Pattern of vegetation change through time

Our palaeoenvironmental record shows that the site of CEN-17.4 has changed dramatically since the beginning of peat accumulation. The early peatland was characterised by a frequently inundated floodplain environment, dominated by Cyperaceae, Poaceae, and an aquatic plant producing *Alisma*-type pollen, possibly *Ranalisma* sp. At the start of the Holocene the vegetation shifted to *Manilkara*-type dominated, possibly seasonally inundated forest. After 9670 cal BP, a mixed swamp forest replaced the *Manilkara*-type forest and has remained in place ever since, with at times substantial variations in the relative proportions of taxa. In particular, there is a long-term trend towards greater abundance of *Raphia*, *Pandanus* and *Symphonia globulifera*, perhaps reflecting slow successional processes; the driest climatic conditions at ~2000 cal BP are associated with a marked increase in heliophiles including *Lophira* (supporting existing narratives around vegetation change during the LHRC); and throughout the record there are high-frequency fluctuations in the relative abundance of pollen taxa, which may simply reflect stochastic ecological processes.

6.3. Fire history and human impact

Fire was prevalent in the grass-sedge vegetation of the early peatland. Plausibly, these fires were lightning-ignited, natural events, but we cannot exclude the possibility that these open grass-dominated wetlands were burned in the dry season by humans, perhaps to facilitate hunting and fishing. Fire activity appears to have all but ceased once the peat swamp forest became established at the start of the Holocene. Moderate peaks in macroscopic charcoal in Zone V likely represent isolated fire occurrences of local extent only. There is no evidence anywhere in our record that the peat itself burned. Likewise, the brief expansion of *Elaeis* in the record is not an unequivocal indicator of human impact. The absence of evidence for human impact does not of course prove that humans were not present, and they may have shaped the environment in ways that are invisible to the proxy techniques employed here (e.g. hunting, digging access canals [Blake, 1993]).

6.4. Climate versus autogenic drivers of ecosystem change

The pattern of ecosystem change in the early part of our record – the shift from open vegetation, to *Manilkara*-type dominated flooded forest, to mineral-poor, mixed swamp forest – is consistent with the pattern of successional change frequently observed in peatlands in similar topographic settings (e.g. Phillips et al., 1997; Roucoux et al., 2013; Kelly et al., 2020). The geochemical data suggest that the degree of flooding with mineral-rich water gradually declined over time, and as the peat built up it is likely that the depth and frequency of flooding by river water declined. This autogenic process alone may have been sufficient to drive the major variation in our record (Zones I to III). However, our data also indicate that peat accumulation and forest structure and composition have been sensitive to past climatic change. Most significantly, the substantial decline in precipitation culminating at ~2000 cal BP that caused the mineralization of several metres of peat is associated with a substantial change in the composition of the forest, including an increase in the abundance of taxa indicating drier and more open conditions (notably *Lophira*). Peat accumulation and the composition of the swamp forest both recovered after this event. Together with the limited evidence for directional successional vegetation change since ~9670 cal BP and the absence of evidence for human impact, our data suggest that changes in precipitation (and possibly its seasonality) have been an important driver of ecological change at the CEN-17.4 site at least since the mixed swamp forest was established ~9670 cal BP, if not before.

This first palaeoenvironmental record from the CCB peatlands has substantially revised our understanding of the timing and pattern of peat initiation, which is now known to be much older and more variable than thought by Dargie et al. (2017). We have shown that the ecosystem at the site today has changed substantially over time, partly following autogenic processes, but also reacting substantially to past climatic change. Further research is required to improve our understanding of the spatio-temporal patterning within the enormous peatland complex at Ekolongouma, and to test whether Ekolongouma is representative of peatlands elsewhere within the CCB.

Author contributions

S.L.L. and I.T.L. conceived the study. G.D., Y.E.B., S.A.I., I.T.L. and S.L.L. collected the cores. D.H. and I.T.L. developed the study. D.H., I.T.L., Y.G., E.S., W.H., G.T., A.B.., J.A.J.S., S.S. and P.G. conducted the laboratory analyses. D.H., I.T.L., Y.G. and E.S. compiled and analysed the data. D.H., I.T.L., G.C.D., Y.G., E.S., W.H., G.T., G.E.B., A.B., P.G., S.E.P., D.M.Y., K.H.R. and S.L.L. interpreted the data. D.H. and I.T.L.

wrote the paper, with input from all co-authors.

Funding

The core collection fieldwork was funded by the Royal Society, to S.L.L., Philip Leverhulme Prize to S.L.L. and a NERC CASE award to S.L.L. and G.C.D. The laboratory analysis, data analysis and write-up was funded by CongoPeat, a NERC Large Grant (NE/R016860/1) to S.L.L., I.T.L., A.B., S.E.P., P.G., supporting D.H., G.T., G.C.D., W.H., G.E.B., and Y.E.B.; and NERC Radiocarbon Facility grant (alloc. no. 1688.0313 and 1797.0414) to I.T.L., S.L.L. and G.C.D. Y. G. was supported by the Agence Nationale de la Recherche (ANR) grant ANR-19-CE01-0022. E.S. was supported by the Deutsche Forschungsgemeinschaft (DFG) grant SCHE 903/19–1 and the DFG-Cluster of Excellence 'The Ocean in the Earth System' at MARUM.

Declaration of competing interest

The authors declare that they have no known competing financial interests or personal relationships that could have appeared to influence the work reported in this paper.

Data availability

The data will be archived in PANGAEA; Data Publisher for Earth & Environmental Science (pangaea.de)

Acknowledgements

We thank the government of the Republic of the Congo, particularly the Minister of Environment, Sustainable Development and the Congo Basin, the Ministry for Research, and the governor of the Likouala Department for permission to sample in the peatlands and for support. We thank the villages of Itanga and Ekolongouma who hosted our field campaigns in Republic of the Congo; R. Mobongo, F. Twagirashyaka, P. Telfer, and B. Evans, and the Wildlife Conservation Society Congo Programme for logistical support; and Marien N'Gouabi University for ongoing advice and support, particularly J. Loumeto and F. Koubouana in Republic of the Congo. We thank P. Abia, T. Angohouni, I. Mokondo, M. Iwango, A. Mobembe, G. N'Gongo, R. Molayei, B. Elongo (Bolembe and Ekolongouma villages) and J.-B. Bobetolo, C. Fatty, Chancel, E.B. Moniobo Belen Ekous, L. Mandomba Landry, F. Mouapeta Fulgence (Itanga village), B. Bongwemisa, J. Sando, J.- P. Lokila, P. Bosange, F. Mongonga, R. Kendewa, E. Mampuya and M. Mbemba for field assistance in collecting the peat cores in Republic of the Congo. We thank C. Kiahtipes and D. Harris for assistance with the pollen taxonomy; the Tropical Wetlands Consortium group and the wider CongoPeat Network for useful discussions; R. Kreutz for laboratory support and H. Plante for U.K. logistical support.

Appendix A. Extended Data Table

Radiocarbon dates from peat cores reported in the text and used to generate age-depth models and net peat accumulation rates.

Core	Depth (cm)	Unique ID	Material	^{14}C age (yr BP)	^{14}C age error (yr)	Median Age (cal BP)	Age range (95%)
CEN-17.4	0.5	AWI-2567.1.1	Fine fraction (<150 μm)	565	170	540	0–899
CEN-17.4	12.8	AWI-1820.1.1	Fine fraction (<150 μm)	345	60	390	158–500
CEN-17.4	53.6	AWI-2255.2.1	Fine fraction (<150 μm)	835	25	713	676–768
CEN-17.4	94.4	AWI-2568.1.1	Fine fraction (<150 μm)	1240	75	1134	974–1282
CEN-17.4	132.5	AWI-2802.1.2	Fine fraction (<150 μm)	1760	70	1641	1427–1826
CEN-17.4	151.5	AWI-1821.1.1	Fine fraction (<150 μm)	2120	60	2069	1893–2306
CEN-17.4	170.5	AWI-2256.2.1	Fine fraction (<150 μm)	4450	30	5031	4872–5279
CEN-17.4	190.5	AWI-2569.1.1	Fine fraction (<150 μm)	6770	85	7610	7431–7776
CEN-17.4	214.4	AWI-2570.1.1	Fine fraction (<150 μm)	7630	95	8413	8197–8591
CEN-17.4	235.6	AWI-2571.1.1	Fine fraction (<150 μm)	7640	110	8424	8183–8635
CEN-17.4	256.5	AWI-2257.2.1	Fine fraction (<150 μm)	7570	35	8370	8213–8419
CEN-17.4	296.5	AWI-1677.2.1	Fine fraction (<150 μm)	8020	140	8864	8482–9286
CEN-17.4	356.5	AWI-2803.1.1	Fine fraction (<150 μm)	9140	50	10,285	10,196–10485
CEN-17.4	396.5	AWI-2258.2.1	Fine fraction (<150 μm)	8360	35	9361	9148–9473
CEN-17.4	418.5	AWI-2572.1.1	Fine fraction (<150 μm)	9930	40	11,301	11,215–11608
CEN-17.4	460.5	AWI-1822.1.1	Fine fraction (<150 μm)	10,150	50	11,751	11,357–11936
CEN-17.4	498.5	AWI-2573.1.1	Fine fraction (<150 μm)	12,450	40	14,569	14,293–14913
CEN-17.4	540.5	AWI-2259.1.1	Fine fraction (<150 μm)	13,650	45	16,463	16,299–16637
CEN-17.4	579.7	AWI-2574.1.1	Fine fraction (<150 μm)	14,750	85	18,051	17,824–18233
CEN-17.4	596.4	AWI-1823.1.1	Fine fraction (<150 μm)	11,550	55	13,401	13,303–13567
CEN-17.4	599.1	AWI-2575.1.1	Fine fraction (<150 μm)	16,850	85	20,350	20,116–20534
CEN-17.4	625.2	AWI-1824.1.2	Fine fraction (<150 μm)	14,050	55	17,071	16,931–17330
EKGkm4	57	SUERC-49356	Fine fraction (<200 μm)	2649	37	2753	2717–2847
EKGkm4	107	SUERC-49357	Fine fraction (<200 μm)	7652	42	8420	8375–8535
EKGkm4	147	SUERC-49358	Fine fraction (<200 μm)	8484	41	9490	9430–9535
EKGkm7-2015	57	SUERC-49354	Fine fraction (<200 μm)	2547	37	2596	2471–2746
EKGkm7-2015	117	SUERC-49355	Fine fraction (<200 μm)	7600	38	8385	8230–8450
EKGkm7-2015	237	SUERC-49351	Fine fraction (<200 μm)	9091	39	10,230	10,180–10335
EKGkm9	57	SUERC-49348	Fine fraction (<200 μm)	1571	35	1439	1364–1525
EKGkm9	67	SUERC-56133	Fine fraction (<200 μm)	1754	38	1634	1543–1706
EKGkm9	77	SUERC-56134	Fine fraction (<200 μm)	1720	35	1596	1533–1699
EKGkm9	87	SUERC-56135	Fine fraction (<200 μm)	702	36	635	558–676
EKGkm9	97	SUERC-49349	Fine fraction (<200 μm)	4811	37	5520	5335–5590
EKGkm9	127	SUERC-56138	Fine fraction (<200 μm)	4251	37	4750	4622–4863
EKGkm9	167	SUERC-56139	Fine fraction (<200 μm)	6354	39	7260	7165–7410
EKGkm9	197	SUERC-56140	Fine fraction (<200 μm)	7662	39	8430	8380–8535
EKGkm9	237	SUERC-56141	Fine fraction (<200 μm)	7993	40	8845	8650–8990
EKGkm9	270	SUERC-49350	Fine fraction (<200 μm)	9340	41	10,525	10,310–10660
ITGkm6	190	SUERC-56869	Fine fraction (<200 μm)	8575	46	9530	9470–9655

Appendix B. Extended organic and inorganic geochemistry methods

Organic geochemistry

Changes in hydroclimate in core CEN-17.4 were derived from $\delta D_{n\text{-}C29}$ (Garcin et al., 2022) reflecting changes in the isotopic composition of precipitation (Sachse et al., 2012; Ladd et al., 2021), which is negatively correlated with precipitation amount in Central Africa (Collins et al., 2013; Garcin et al., 2018). Additionally to the isotopic composition of the precipitation, $\delta D_{n\text{-}C29}$ can be influenced by isotopic D-enrichment due to soil evaporation/evapotranspiration together with changes in vegetation types and related to plant life forms and photosynthetic pathways (Sachse et al., 2012). For example, previously described apparent fractionation (ε) between precipitation and *n*-alkane was −129 ± 22‰ for C_3 plants (ε_{C3}; Feakins et al. (2016)) and −145 ± 20‰ for C_4 plants (ε_{C4}; Smith and Freeman (2006)). As the $\delta^{13}C_{n\text{-}C29}$ values of the CEN-17.4 core show significant variations (from −24.5‰ to −36‰) during the late Pleistocene/Holocene transition, a correction of the vegetation effect on the $\delta D_{n\text{-}C29}$ values should be considered. By using paired $\delta^{13}C_{n\text{-}C29}$ values, the effect of changing vegetation on $\delta D_{n\text{-}C29}$ values can be assessed as previously determined (Collins et al., 2013; Feakins, 2013; Shanahan et al., 2015; Tierney et al., 2017; Garcin et al., 2018). Following those studies, we first derived the relative contribution of C_3 plant waxes (f_{C3}) to the peat from the $\delta^{13}C_{n\text{-}C29}$ values by using a linear binary mixing model with end-member values for C_3 plants ($\delta^{13}C_{C3}$) and C_4 plants ($\delta^{13}C_{C4}$) taken from the "All Africa" compilation of Garcin et al. (2014) as follows:

$$\delta^{13}C_{n-C29} = (f_{C3})\delta^{13}C_{C3} + (1 - f_{C3})\delta^{13}C_{C4} \quad (1)$$

Solving for f_{C3} equation (1) becomes:

$$f_{C3} = \frac{\delta^{13}C_{n-C29} + \delta^{13}C_{C4}}{\delta^{13}C_{C4} - \delta^{13}C_{C3}} \quad (2)$$

Second, we estimated peat ε as follows:

$$\varepsilon_{=}(f_{C3})\varepsilon_{C3} + (1 - f_{C3})\varepsilon_{C4} \quad (3)$$

Third, we subtracted ε from $\delta D_{n\text{-}C29}$ to obtain $\delta D_{n\text{-}C29\text{-}vcorr}$:

$$\delta D_{n-C29-vcorr=} \left[\frac{\delta D_{n-C29} + 1000}{\left(\frac{\varepsilon}{1000}\right) + 1} \right] - 1000 \quad (4)$$

Global ice volume changes can further affect isotopes in the hydrological cycle (Waelbroeck et al., 2002). Similarly to Shanahan et al. (2015) and Tierney et al. (2017), we corrected for this effect assuming a 1‰ change in $\delta^{18}O$ at the Last Glacial Maximum (Shackleton, 2000; Waelbroeck et al., 2002) and a deuterium excess of zero for the ocean water (Vimeux et al., 2001; Tierney et al., 2011). We established a time series of $\delta^{18}O_{ocean}$ values for the last 18,000 years by scaling these changes to the benthic oxygen isotope data from Waelbroeck et al. (2002). Changes in δD_{ocean} derived from $\delta^{18}O_{ocean}$ were subsequently subtracted from $\delta D_{n\text{-}C29\text{-}vcorr}$ values to produce $\delta D_{n\text{-}C29}$ values corrected from both vegetation and ice volume ($\delta D_{n\text{-}C29\text{-}v\&icecorr}$) as follows:

$$\delta D_{n-C29-v\&icecorr=} \left[\frac{\delta D_{n-C29-vcorr} + 1000}{\left(\frac{8.\delta^{18}O_{ocean}}{1000}\right) + 1} \right] - 1000 \quad (5)$$

Inorganic geochemistry

Peat samples were dried at 65 °C for 4 days then finely milled using agate grinding jars and balls. Approximately 200 mg of the milled sample was digested with 8 ml of HNO_3 (67–69% trace element grade) at room temperature for 24 h; 2 ml of H_2O_2 was then added, left overnight, then heated at 95 °C for 2 h. After cooling for 30 min, Milli-Q water was added up to 50 ml final volume. Diluted samples were allowed to settle for 30 min before filtering with 0.22 μm polyethersulfone membrane syringe filters. Each digestion batch contained three blanks and ten blank digestions were used to estimate limits of detection (LOD). For ICP-MS analysis, 1 ml of the digested sample was diluted with 9 ml of Milli-Q water. Multi-element analysis of diluted solutions was undertaken by ICP-MS (Thermo-Fisher Scientific iCAP-Q; Thermo Fisher Scientific, Bremen, Germany). The instrument was run employing three operational modes, including (i) a collision-cell (Q cell) using He with kinetic energy discrimination (He-cell) to remove polyatomic interferences, (ii) standard mode (STD) in which the collision cell is evacuated and (iii) hydrogen mode (H_2-cell) in which H_2 gas is used as the cell gas. Samples were introduced from an autosampler (Cetac ASX-520) incorporating an ASXpress™ rapid uptake module through a PEEK nebulizer (Burgener Mira Mist). Internal standards were introduced to the sample stream on a separate line via the ASXpress unit and included Sc (125 ppb), Ge (55 ppb), Rh (5 ppb) and Ir (2.5 ppb) in 2% trace analysis grade (Fisher Scientific, UK) HNO_3. External multi-element calibration standards (Claritas-PPT grade CLMS-2 from SPEX Certiprep Inc., Metuchen, NJ, USA) included Ag, Al, As, Ba, Be, Cd, Ca, Co, Cr, Cs, Cu, Fe, K, Li, Mg, Mn, Mo, Na, Ni, P, Pb, Rb, S, Se, Sr, Ti, Tl, U, V and Zn, in the range 0–100 ppb (0, 20, 40, 100 ppb). A bespoke external multi-element calibration solution (PlasmaCAL, SCP Science, France) was used to create Ca, Mg, Na and K standards in the range 0–30 mg L^{-1}. Calibration for P, B and S utilized in-house standard solutions (KH_2PO_4, K_2SO_4 and H_3BO_3). In-sample switching was used to measure B and P in STD mode, Se in H_2-cell mode and all other elements in He-cell mode. Sample processing was undertaken using Qtegra™ software (Thermo-Fisher Scientific) utilizing external cross-calibration between pulse-counting and analogue detector modes when required.

References

Abràmoff, M.D., Magalhães, P.J., Ram, S.J., 2004. Image processing with ImageJ. Biophot. Int. 11 (7), 36–42.

Adjanohoun, E.J., et al., 1988. –- Contribution aux études ethnobotaniques et floristiques en République Populaire du Congo. ACCT, Paris, p. 605p.

African Plant Database (version 3.4.0). Conservatoire et Jardin botaniques de la Ville de Genève and South African National Biodiversity Institute, Pretoria. Retrieved from http://africanplantdatabase.ch.

Aleman, J.C., Blarquez, O., Elenga, H., Paillard, J., Kimpuni, V., Itoua, G., Issele, G., Staver, A.C., 2019. Palaeo-trajectories of forest savannization in the southern Congo. Biol. Lett. 15 (8), 20190284. https://doi.org/10.1098/rsbl.2019.0284.

Andersen, S.T., 1974. Wind conditions and pollen deposition in a mixed deciduous forest: I. Wind conditions and pollen dispersal. Grana 14 (2–3), 57–63. https://doi.org/10.1080/00173137409429894.

Anderson, J.A.R., 1983. The tropical peat swamps of western Malesia. In: Gore, A.J.P. (Ed.), Ecosystems of the World 4B: Mires: Swamp, Bog, Fen and Moor. Elsevier, Amsterdam, pp. 181–199.

Anderson, J.A.R., Muller, J., 1975. Palynological study of a Holocene peat and a Miocene coal deposit from NW Borneo. Rev. Palaeobot. Palynol. 19 (4), 291–351. https://doi.org/10.1016/0034-6667(75)90049-4.

Andrews, J.T., Voelker, A.H.L., 2018. Heinrich events" (and sediments): a history of terminology and recommendations for future usage. Quat. Sci. Rev. 187, 31–40.

Argue, C.L., 1974. Pollen studies in the Alismataceae (Alismaceae). Bot. Gaz. 135 (4), 338–344. https://doi.org/10.1086/336770.

Bayon, G., Dennielou, B., Etoubleau, J., Ponzevera, E., Toucanne, S., Bermell, S., 2012. Intensifying weathering and land use in iron age central Africa. Science 335 (6073), 1219–1222. https://doi.org/10.1126/science.1215400.

Bayon, G., Schefuß, E., Dupont, L., Borges, A.V., Dennielou, B., Lambert, T., Mollenhauer, G., Monin, L., Ponzevera, E., Skonieczny, C., André, L., 2019. The

roles of climate and human land-use in the late Holocene rainforest crisis of Central Africa. Earth Planet Sci. Lett. 505, 30–41. https://doi.org/10.1016/j.epsl.2018.10.016.
Bengo, M.D., Elenga, H., Maley, J., Giresse, P., 2020. Evidence of pollen transport by the Sanaga River on the Cameroon shelf. Compt. Rendus Geosci. 352 (1), 59–72. https://doi.org/10.5802/crgeos.1.
Bennett, K.D., 1996. Determination of the number of zones in a biostratigraphical sequence. New Phytol. 132 (1), 155–170. https://doi.org/10.1111/j.1469-8137.1996.tb04521.x.
Birks, H.J.B., Gordon, A.D., 1985. Numerical Methods in Quaternary Pollen Analysis. Academic Press, London.
Blaauw, M., Christen, J.A., 2011. Flexible paleoclimate age-depth models using an autoregressive gamma process. Bayesian Anal. 6 (3), 457–474. https://doi.org/10.1214/ba/1339616472.
Blake, S., 1993. A Reconnaissance Survey in the Likouala Swamps of Northern Congo and its Implications for Conservation. Doctoral dissertation, University of Edinburgh.
Blei, D.M., Lafferty, J.D., 2007. A correlated topic model of science. Ann. Appl. Stat. 1 (1), 17–35. https://doi.org/10.1214/07-AOAS114.
Bocko, Y.E., Dargie, G., Ifo, S.A., Yoka, J., Loumeto, J.J., 2016. Répartition spatiale de la richesse floristique des forêts marécageuses de la Likouala, Nord-Congo. Afr. Sci. 12 (4), 200–212.
Bostoen, K., Grollemund, R., Muluwa, J.K., 2013. Climate-induced vegetation dynamics and the Bantu Expansion: evidence from Bantu names for pioneer trees (Elaeis guineensis, Canarium schweinfurthii, and Musanga cecropioides). Compt. Rendus Geosci. 345 (7–8), 336–349. https://doi.org/10.1016/j.crte.2013.03.005.
Bouillenne, R., Moureau, J., Deuse, P., 1955. Esquisse écologique des faciès forestiers et marécageux des bords du lac Tumba:(Domaine de l'IRSAC, Mabali, Congo belge), vol. 3. Académie royale des sciences coloniales.
Bremond, L., Oslisly, R., Sebag, D., Bentaleb, I., Favier, C., Henga-Botsikabobe, K., Mvoubou, M., Ngomanda, A., de Saulieu, G., Ecotrop Team, 2021. Establishment and functioning of the savanna marshes of the Lopé National Park in Gabon since the termination of the African humid period and the arrival of humans 2500 years ago. Holocene 31 (7), 1186–1196. https://doi.org/10.1177/09596836211003230.
Brncic, T.M., Willis, K.J., Harris, D.J., Washington, R., 2007. Culture or climate? The relative influences of past processes on the composition of the lowland Congo rainforest. Phil. Trans. Biol. Sci. 362 (1478), 229–242. https://doi.org/10.1098/rstb.2006.1982.
Brncic, T.M., Willis, K.J., Harris, D.J., Telfer, M.W., Bailey, R.M., 2009. Fire and climate change impacts on lowland forest composition in northern Congo during the last 2580 years from palaeoecological analyses of a seasonally flooded swamp. Holocene 19 (1), 79–89. https://doi.org/10.1177/0959683608098954.
Burrows, C.J., 1990. Processes of vegetation change. In: Processes of Vegetation Change. Springer, Dordrecht, pp. 359–419. https://doi.org/10.1007/978-94-011-3058-5_11.
Bwangoy, J.R.B., Hansen, M.C., Roy, D.P., De Grandi, G., Justice, C.O., 2010. Wetland mapping in the Congo Basin using optical and radar remotely sensed data and derived topographical indices. Rem. Sens. Environ. 114 (1), 73–86. https://doi.org/10.1016/j.rse.2009.08.004.
Campbell, D., 2005. The Congo River Basin. In: The World's Largest Wetlands: Ecology and Conservation. Cambridge University Press, Cambridge (United Kingdom), pp. 149–165.
Christian, H.J., Blakeslee, R.J., Boccippio, D.J., Boeck, W.L., Buechler, D.E., Driscoll, K.T., Goodman, S.J., Hall, J.M., Koshak, W.J., Mach, D.M., Stewart, M.F., 2003. Global frequency and distribution of lightning as observed from space by the Optical Transient Detector. J. Geophys. Res. Atmos. 108 (D1). https://doi.org/10.1029/2002JD002347. ACL-4.
Clark, J.S., 1988. Stratigraphic charcoal analysis on petrographic thin sections: application to fire history in northwestern Minnesota. Quat. Res. 30 (1), 81–91. https://doi.org/10.1016/0033-5894(88)90089-0.
Cobb, A.R., Harvey, C.F., 2019. Scalar simulation and parameterization of water table dynamics in tropical peatlands. Water Resour. Res. 55 (11), 9351–9377. https://doi.org/10.1029/2019WR025411.
Collins, J.A., Schefuß, E., Mulitza, S., Prange, M., Werner, M., Tharammal, T., Paul, A., Wefer, G., 2013. Estimating the hydrogen isotopic composition of past precipitation using leaf-waxes from western Africa. Quat. Sci. Rev. 65, 88–101. https://doi.org/10.1016/j.quascirev.2013.01.007.
Collins, J.A., Prange, M., Caley, T., Gimeno, L., Beckmann, B., Mulitza, S., Skonieczny, C., Roche, D., Schefuß, E., 2017. Rapid termination of the African Humid Period triggered by northern high-latitude cooling. Nat. Commun. 8 (1), 1–11. https://doi.org/10.1038/s41467-017-01454-y.
Cook, K.H., Liu, Y., Vizy, E.K., 2020. Congo Basin drying associated with poleward shifts of the African thermal lows. Clim. Dynam. 54 (1–2), 863–883. https://doi.org/10.1007/s00382-019-05033-3.
Crezee, B., Dargie, G.C., Ewango, C.E., Mitchard, E.T., Emba B, O., Kanyama T, J., Bola, P., Ndjango, J.B.N., Girkin, N.T., Bocko, Y.E., Ifo, S.A., 2022. Mapping peat thickness and carbon stocks of the central Congo Basin using field data. Nat. Geosci. 15 (8), 639–644.
Crosby, A.G., Fishwick, S., White, N., 2010. Structure and evolution of the intracratonic Congo Basin. G-cubed 11 (6). https://doi.org/10.1029/2009GC003014.
Dargie, G.C., 2015. Quantifying and Understanding the Tropical Peatlands of the Central Congo Basin. Doctoral dissertation, University of Leeds.
Dargie, G.C., Lewis, S.L., Lawson, I.T., Mitchard, E.T., Page, S.E., Bocko, Y.E., Ifo, S.A., 2017. Age, extent and carbon storage of the central Congo Basin peatland complex. Nature 542 (7639), 86–90. https://doi.org/10.1038/nature21048.
Dargie, G.C., Lawson, I.T., Rayden, T.J., Miles, L., Mitchard, E.T., Page, S.E., Bocko, Y.E., Ifo, S.A., Lewis, S.L., 2019. Congo Basin peatlands: threats and conservation priorities. Mitig. Adapt. Strategies Glob. Change 24 (4), 669–686. https://doi.org/10.1007/s11027-017-9774-8.
Davenport, I.J., McNicol, I., Mitchard, E.T., Dargie, G., Suspense, I., Milongo, B., Bocko, Y.E., Hawthorne, D., Lawson, I., Baird, A.J., Page, S., 2020. First evidence of peat domes in the Congo basin using LiDAR from a fixed-wing drone. Rem. Sens. 12 (14), 2196. https://doi.org/10.3390/rs12142196.
De Wit, M.J., Guillocheau, F., De Wit, M.C. (Eds.), 2015. Geology and Resource Potential of the Congo Basin. Springer Science & Business Media. https://doi.org/10.1007/978-3-642-29482-2.
Delvaux, D., Maddaloni, F., Tesauro, M., Braitenberg, C., 2021. The Congo Basin: stratigraphy and subsurface structure defined by regional seismic reflection, refraction and well data. Global Planet. Change 198, 103407. https://doi.org/10.1016/j.gloplacha.2020.103407.
deMenocal, P., Ortiz, J., Guilderson, T., Adkins, J., Sarnthein, M., Baker, L., Yarusinsky, M., 2000. Abrupt onset and termination of the African Humid Period: rapid climate responses to gradual insolation forcing. Quat. Sci. Rev. 19, 347–361. https://doi.org/10.1016/S0277-3791(99)00081-5.
Deuse, P., 1960. Étude écologique et phytosociologique de la végétation des" esobe" de la région Est du lac Tumba:(Congo belge). Académie royale des sciences d'outre-mer.
Dohong, A., Aziz, A.A., Dargusch, P., 2017. A review of the drivers of tropical peatland degradation in South-East Asia. Land Use Pol. 69, 349–360. https://doi.org/10.1016/j.landusepol.2017.09.035.
Dommain, R., Couwenberg, J., Joosten, H., 2011. Development and carbon sequestration of tropical peat domes in south-east Asia: links to post-glacial sea-level changes and Holocene climate variability. Quat. Sci. Rev. 30 (7–8), 999–1010. https://doi.org/10.1016/j.quascirev.2011.01.018.
Dufrêne, M., Legendre, P., 1997. Species assemblages and indicator species: the need for a flexible asymmetrical approach. Ecol. Monogr. 67, 345–366. https://doi.org/10.1890/0012-9615(1997)067[0345:SAAIST]2.0.CO, 2.
Elenga, H., 1992. Végétation et climat du Congo depuis 24 000 ans B. P: analyse palynologique de séquences sédimentaires du Pays Bateke et du littoral, vol. 3. Doctoral dissertation, Aix-Marseille.
Elenga, H., Vincens, A., Schwartz, D., 1991. Présence d'éléments forestiers montagnards sur les Plateaux Batéké (Congo) au Pléistocène supérieur: nouvelles données palynologiques. In: Symposium on African Palynology, pp. 239–252.
Elenga, H., Schwartz, D., Vincens, A., 1994. Pollen evidence of late Quaternary vegetation and inferred climate changes in Congo. Palaeogeogr. Palaeoclimatol. Palaeoecol. 109 (2–4), 345–356. https://doi.org/10.1016/0031-0182(94)90184-8.
Elenga, H., Schwartz, D., Vincens, A., Bertaux, J., de Namur, C., Martin, L., Wirrmann, D., Servant, M., 1996. Diagramme pollinique holocène du lac Kitina (Congo): mise en évidence de changements paléobotaniques et paléoclimatiques dans le massif forestier du Mayombe. In: Comptes Rendus de l'Académie de Sciences. Série IIa: Sciences de la Terre et des Planètes, pp. 403–410.
Elenga, H., de Namur, C., Vincens, A., Roux, M., Schwartz, D., 2000. Use of plots to define pollen-vegetation relationships in densely forested ecosystems of tropical Africa. Rev. Palaeobot. Palynol. 112 (1–3), 79–96. https://doi.org/10.1016/S0034-6667(00)00036-1.
Elenga, H., Maley, J., Vincens, A., Farrera, I., 2004. Palaeoenvironments, Palaeoclimates and Landscape Development in Atlantic Equatorial Africa: a Review of Key Sites Covering the Last 25 Kyrs. *Past Climate Variability through Europe And Africa*, pp. 181–198. https://doi.org/10.1007/978-1-4020-2121-3_10.
Évrard, C., 1968. *Recherches écologiques sur le peuplement forestier des sols hydromorphes de la Cuvette centrale congloaise* (No. 110). Institut pour l'étude agronomique du Congo.
Fay, J.M., Agnagna, M., Moore, J., Oko, R., 1989. Gorillas (Gorilla gorilla gorilla) in the Likouala swamp forests of north central Congo: preliminary data on populations and ecology. Int. J. Primatol. 10 (5), 477–486. https://doi.org/10.1007/BF02736372.
Feakins, S.J., 2013. Pollen-corrected leaf wax D/H reconstructions of northeast African hydrological changes during the late Miocene. Palaeogeogr. Palaeoclimatol. Palaeoecol. 374, 62–71. https://doi.org/10.1016/j.palaeo.2013.01.004.
Feakins, S.J., Bentley, L.P., Salinas, N., Shenkin, A., Blonder, B., Goldsmith, G.R., Ponton, C., Arvin, L.J., Wu, M.S., Peters, T., West, A.J., Martin, R.E., Enquist, B.J., Asner, G.P., Malhi, Y., 2016. Plant leaf wax biomarkers capture gradients in hydrogen isotopes of precipitation from the Andes and Amazon. Geochem. Cosmochim. Acta 182, 155–172. https://doi.org/10.1016/j.gca.2016.03.018.
Garcin, Y., Schefuß, E., Schwab, V.F., Garreta, V., Gleixner, G., Vincens, A., Todou, G., Séné, O., Onana, J.-M., Achoundong, G., Sachse, D., 2014. Reconstructing C3 and C4 vegetation cover using n-alkane carbon isotope ratios in recent lake sediments from Cameroon, Western Central Africa. Geochem. Cosmochim. Acta 142, 482–500. https://doi.org/10.1016/j.gca.2014.07.004.
Garcin, Y., Deschamps, P., Ménot, G., de Saulieu, G., Schefuß, E., Sebag, D., Dupont, L., Oslisly, R., Brademann, B., Mbusnum, K.G., Onana, J.-M., Ako, A.A., Epp, L.S., Tjallingii, R., Strecker, M.R., Brauer, A., Sachse, D., 2018. Early anthropogenic impact on Western Central African rainforests 2,600 y ago. Proc. Natl. Acad. Sci. U.S.A. 115, 3261–3266. https://doi.org/10.1073/pnas.1715336115.
Garcin, Y., Schefuß, E., Dargie, G.C., Hawthorne, D., Lawson, I.T., Sebag, D., Biddulph, G.E., Crezee, B., Bocko, Y.E., Ifo, S.A., Mampouya Wenina, Y.E., et al., 2022. Hydroclimatic vulnerability of peat carbon in the central Congo Basin.

Nature 1–6. https://doi.org/10.1038/s41586-022-05389-3.
Gasse, F., 2000. Hydrological changes in the African tropics since the last glacial maximum. Quat. Sci. Rev. 19 (1–5), 189–211. https://doi.org/10.1016/S0277-3791(99)00061-X.
Giresse, P., Maley, J., Brenac, P., 1994. Late Quaternary palaeoenvironments in the Lake Barombi Mbo (West Cameroon) deduced from pollen and carbon isotopes of organic matter. Palaeogeogr. Palaeoclimatol. Palaeoecol. 107 (1–2), 65–78. https://doi.org/10.1016/0031-0182(94)90165-1.
Giresse, P., Mvoubou, M., Maley, J., Ngomanda, A., 2009. Late-Holocene equatorial environments inferred from deposition processes, carbon isotopes of organic matter, and pollen in three shallow lakes of Gabon, west-central Africa. J. Paleolimnol. 41 (2), 369–392. https://doi.org/10.1007/s10933-008-9231-5.
Giresse, P., Maley, J., Chepstow-Lusty, A., 2020. Understanding the 2500 yr BP rainforest crisis in West and central Africa in the framework of the late Holocene: pluridisciplinary analysis and multi-archive reconstruction. Global Planet. Change, 103257. https://doi.org/10.1016/j.gloplacha.2020.103257.
Goossens, D., 2008. Techniques to measure grain-size distributions of loamy sediments: a comparative study of ten instruments for wet analysis. Sedimentology 55 (1), 65–96.
Hamilton, A.A., Taylor, D., 1991. History of climate and forests in tropical Africa during the last 8 million years. In: Tropical Forests and Climate. Springer, Dordrecht, pp. 65–78. https://doi.org/10.1007/978-94-017-3608-4_8.
Hapsari, K.A., Biagioni, S., Jennerjahn, T.C., Reimer, P.M., Saad, A., Achnopha, Y., Sabiham, S., Behling, H., 2017. Environmental dynamics and carbon accumulation rate of a tropical peatland in Central Sumatra, Indonesia. Quat. Sci. Rev. 169, 173–187. https://doi.org/10.1016/j.quascirev.2017.05.026.
Hawthorne, D., Mustaphi, C.J.C., Aleman, J.C., Blarquez, O., Colombaroli, D., Daniau, A.L., Marlon, J.R., Power, M., Vanniere, B., Han, Y., Hantson, S., 2018. Global Modern Charcoal Dataset (GMCD): a tool for exploring proxy-fire linkages and spatial patterns of biomass burning. Quat. Int. 488, 3–17. https://doi.org/10.1016/j.quaint.2017.03.046.
He, F., Shakun, J.D., Clark, P.U., Carlson, A.E., Liu, Z., Otto-Bliesner, B.L., Kutzbach, J.E., 2013. Northern Hemisphere forcing of Southern Hemisphere climate during the last deglaciation. Nature 494, 81–85. https://doi.org/10.1038/nature11822.
Heiri, O., Lotter, A.F., Lemcke, G., 2001. Loss on ignition as a method for estimating organic and carbonate content in sediments: reproducibility and comparability of results. J. Paleolimnol. 25 (1), 101–110. https://doi.org/10.1023/A:1008119611481.
Hemingway, J.D., Schefuß, E., Spencer, R.G., Dinga, B.J., Eglinton, T.I., McIntyre, C., Galy, V.V., 2017. Hydrologic controls on seasonal and inter-annual variability of Congo River particulate organic matter source and reservoir age. Chem. Geol. 466, 454–465. https://doi.org/10.1016/j.chemgeo.2017.06.034.
Henga-Botsikabobe, K., Ngomanda, A., Oslisly, R., Favier, C., Muller, S.D., Bremond, L., 2020. Modern pollen–vegetation relationships within tropical marshes of Lopé National Park (Central Gabon). Rev. Palaeobot. Palynol. 275, 104168. https://doi.org/10.1016/j.revpalbo.2020.104168.
Hewlett, B.S. (Ed.), 2017. Hunter-Gatherers of the Congo Basin: Cultures, Histories, and Biology of African Pygmies. Routledge. https://doi.org/10.4324/9780203789438.
Hogg, A.G., Heaton, T.J., Hua, Q., Palmer, J.G., Turney, C.S., Southon, J., Bayliss, A., Blackwell, P.G., Boswijk, G., Ramsey, C.B., Pearson, C., 2020. SHCal20 Southern Hemisphere calibration, 0-55,000 years cal BP. Radiocarbon 62 (4), 759–778. https://doi.org/10.1017/RDC.2020.59.
Hooijer, A., Page, S., Canadell, J.G., Silvius, M., Kwadijk, J., Wösten, H., Jauhiainen, J., 2010. Current and future CO 2 emissions from drained peatlands in Southeast Asia. Biogeosciences 7 (5), 1505–1514. https://doi.org/10.5194/bg-7-1505-2010.
Householder, J.E., Janovec, J.P., Tobler, M.W., Page, S., Lähteenoja, O., 2012. Peatlands of the Madre de Dios River of Peru: distribution, geomorphology, and habitat diversity. Wetlands 32 (2), 359–368. https://doi.org/10.1007/s13157-012-0271-2.
Hubbell, S.P., Ahumada, J.A., Condit, R., Foster, R.B., 2001. Local neighborhood effects on long-term survival of individual trees in a neotropical forest. Ecol. Res. 16 (5), 859–875. https://doi.org/10.1046/j.1440-1703.2001.00445.x.
Hughes, R.H., 1992. A Directory of African Wetlands. IUCN.
Hughes, P.D.M., 2000. A reappraisal of the mechanisms leading to ombrotrophy in British raised mires. Ecol. Lett. 3 (1), 7–9. https://doi.org/10.1046/j.1461-0248.2000.00118.x.
Hughes, P.D.M., Barber, K.E., 2004. Contrasting pathways to ombrotrophy in three raised bogs from Ireland and Cumbria, England. Holocene 14 (1), 65–77. https://doi.org/10.1191/0959683604hl690rp.
Ifo, S.A., Moutsambote, J.M., Koubouana, F., Yoka, J., Ndzai, S.F., Bouetou-Kadilamio, L.N.O., Mampouya, H., Jourdain, C., Bocko, Y., Mantota, A.B., Mbemba, M., 2016. Tree species diversity, richness, and similarity in intact and degraded forest in the tropical rainforest of the Congo Basin: case of the forest of Likouala in the Republic of Congo. Int. J. Financ. Res. https://doi.org/10.1155/2016/7593681.
Jackson, S.T., Lyford, M.E., 1999. Pollen dispersal models in Quaternary plant ecology: assumptions, parameters, and prescriptions. Bot. Rev. 65 (1), 39–75. https://doi.org/10.1007/BF02856557.
Jansen, J.H.F., Van Weering, T.C., Gieles, R., Van Iperen, J., 1984. Middle and late Quaternary oceanography and climatology of the Zaire-Congo fan and the adjacent eastern Angola Basin. Neth. J. Sea Res. 17 (2–4), 201–249. https://doi.org/10.1016/0077-7579(84)90048-6.
Jansen, F., Ufkes, E., Bey Khelifa, L., 1995. The younger Dryas in equatorial and southern Africa and in the southeast Atlantic Ocean. Younger Dryas 141, 147.
Juggins, S., 2020. Analysis of Quaternary Science Data, R Package Version, 0.9-26. https://cran.r-project.org/package=rioja.
Julier, A.C., Manzano, S., Razanatsoa, E., Razafimanantsoa, A.H., Githumbi, E., Hawthorne, D., Oden, G., Schüler, L., Tossou, M., Bunting, J., 2021. Modern pollen studies from tropical Africa and their use in palaeoecology. In: Quaternary Vegetation Dynamics-The African Pollen Database. CRC Press, pp. 317–348. https://doi.org/10.1201/9781003162766-21.
Kadima, E., Delvaux, D., Sebagenzi, S.N., Tack, L., Kabeya, S.M., 2011. Structure and geological history of the Congo Basin: an integrated interpretation of gravity, magnetic and reflection seismic data. Basin Res. 23 (5), 499–527. https://doi.org/10.1111/j.1365-2117.2011.00500.x.
Kahlheber, S., Eggert, M.K., Seidensticker, D., Wotzka, H.P., 2014. Pearl millet and other plant remains from the early iron age site of Boso-Njafo (inner Congo basin, Democratic Republic of the Congo). Afr. Archaeol. Rev. 31 (3), 479–512. https://doi.org/10.1007/s10437-014-9168-1.
Kelly, T.J., Lawson, I.T., Roucoux, K.H., Baker, T.R., Jones, T.D., Sanderson, N.K., 2017. The vegetation history of an Amazonian domed peatland. Palaeogeogr. Palaeoclimatol. Palaeoecol. 468, 129–141. https://doi.org/10.1016/j.palaeo.2016.11.039.
Kelly, T.J., Lawson, I.T., Roucoux, K.H., Baker, T.R., Coronado, E.N.H., 2020. Patterns and drivers of development in a west Amazonian peatland during the late Holocene. Quat. Sci. Rev. 230, 106168. https://doi.org/10.1016/j.quascirev.2020.106168.
Kiahtipes, C., Lupo, K., Schmitt, D., Ndanga, J.P., Jones, J., Lee, R., 2011. Prehistory and the present. Before Farming 2011 (2), 1–15. https://doi.org/10.3828/bfarm.2011.2.4.
Ladd, S.N., Maloney, A.E., Nelson, D.B., Prebble, M., Camperio, G., Sear, D.A., Hassall, J.D., Langdon, P.G., Sachs, J.P., Dubois, N., 2021. Leaf wax hydrogen isotopes as a hydroclimate proxy in the tropical Pacific. J. Geophys. Res. 126, e2020JG005891. https://doi.org/10.1029/2020JG005891.
Lähteenoja, O., Ruokolainen, K., Schulman, L., Alvarez, J., 2009. Amazonian floodplains harbour minerotrophic and ombrotrophic peatlands. Catena 79 (2), 140–145. https://doi.org/10.1016/j.catena.2009.06.006.
Laraque, A., Pouyaud, B., Rocchia, R., Robin, E., Chaffaut, I., Moutsambote, J.M., Maziezoula, B., Censier, C., Albouy, Y., Elenga, H., Etcheber, H., 1998. Origin and function of a closed depression in equatorial humid zones: the Lake Télé in North Congo. J. Hydrol. 207 (3–4), 236–253. https://doi.org/10.1016/S0022-1694(98)00137-1.
Lebamba, J., Vincens, A., Jolly, D., Ngomanda, A., Schevin, P., Maley, J., Bentaleb, I., 2009. Modern pollen rain in savanna and forest ecosystems of Gabon and Cameroon, Central Atlantic Africa. Rev. Palaeobot. Palynol. 153 (1–2), 34–45. https://doi.org/10.1016/j.revpalbo.2008.06.004.
Lebrun, J., Gilbert, G., 1954. Une classification écologique des forêts du Congo. Institut national pour l'étude agronomique du Congo Belge.
Legendre, P., Birks, H.J.B., 2012. From classical to canonical ordination. In: Tracking Environmental Change Using Lake Sediments. Springer, Dordrecht, pp. 201–248. https://doi.org/10.1007/978-94-007-2745-8_8.
Leng, L.Y., Ahmed, O.H., Jalloh, M.B., 2019. Brief review on climate change and tropical peatlands. Geosci. Front. 10 (2), 373–380. https://doi.org/10.1016/j.gsf.2017.12.018.
Léonard, J., 1996. La végétation pionnière à Ranalisma et Eichhornia des petites rivières en forêt dense dans la région de Yangambi (Kisangani, Zaïre). Bulletin du Jardin botanique national de Belgique/Bulletin van de Nationale Plantentuin van Belgie, pp. 293–330. https://doi.org/10.2307/3668454.
Lewis, J., 2002. Forest Hunter-Gatherers and Their World: a Study of the Mbendjele Yaka Pygmies of Congo-Brazzaville and Their Secular and Religious Activities and Representations. Doctoral Thesis, University of London.
Liu, Z., Otto-Bliesner, B.L., He, F., Brady, E.C., Tomas, R., Clark, P.U., Carlson, A.E., Lynch-Stieglitz, J., Curry, W., Brook, E., Erickson, D., Jacob, R., Kutzbach, J., Cheng, J., 2009. Transient simulation of last deglaciation with a new mechanism for Bølling-Allerød warming. Science 325, 310–314. https://doi.org/10.1126/science.1171041.
Llampazo, G.F., Honorio Coronado, E.N., del Aguila-Pasquel, J., Cordova Oroche, C.J., Díaz Narvaez, A., Reyna Maytahuari, J., Grandez Ríos, J., Lawson, I.T., Hastie, A., Baird, A.J., Baker, T.R., 2022. The presence of peat and variation in tree species composition are under different hydrological controls in Amazonian wetland forests. Hydrol. Process., e14690
MacArthur, R.H., Wilson, E.O., 1967. The Theory of Island Biogeography, vol. 1. Princeton University Press, Princeton, NJ.
Maley, J., 1987. Fragmentation de la forêt dense humide africaine et extension des biotopes montagnards au Quaternaire récent: nouvelles données polliniques et chronologiques. Implications paléoclimatiques et biogéographiques. In: Palaeoecology of Africa and the Surrounding Islands, pp. 307–334.
Maley, J., 1996. Le cadre paléoenvironnemental des refuges forestiers africains: quelques données et hypothèses. In: The Biodiversity of African Plants. Springer, Dordrecht, pp. 519–535. https://doi.org/10.1007/978-94-009-0285-5_68.
Maley, J., 1999. L'expansion du palmier à huile (Elaeis guineensis) en Afrique Centrale au cours des trois derniers millénaires: nouvelles données et interprétations. *L'homme et la Forêt Tropicale*. Travaux Société Ecologie Humaine, Paris, pp. 237–254.
Maley, J., Brenac, P., 1998. Vegetation dynamics, palaeoenvironments and climatic changes in the forests of western Cameroon during the last 28,000 years BP. Rev. Palaeobot. Palynol. 99 (2), 157–187. https://doi.org/10.1016/S0034-6667(97)00047-X.
Maley, J., Chepstow-lusty, A., 2001. Elaeis guineensis Jacq.(oil palm) fluctuations in

central Africa during the late Holocene: climate or human driving forces for this pioneering species? Veg. Hist. Archaeobotany 10 (2), 117–120. https://doi.org/10.1007/PL00006920.
Maley, J., Elenga, H., 1993. The role of clouds in the evolution of tropical African palaeoenvironments. Veille Clim. Satell 46, 51–63.
Maley, J., Doumenge, C., Giresse, P., Mahé, G., Philippon, N., Hubau, W., Lokonda, M.O., Tshibamba, J.M., Chepstow-Lusty, A., 2018. Late Holocene forest contraction and fragmentation in central Africa. Quat. Res. 89, 43–59. https://doi.org/10.1017/qua.2017.97.
Malounguila-Nganga, D., Giresse, P., Boussafir, M., Miyouna, T., 2017. Late Holocene swampy forest of Loango Bay (Congo). Sedimentary environments and organic matter deposition. J. Afr. Earth Sci. 134, 419–434. https://doi.org/10.1016/j.jafrearsci.2017.05.022.
Marengo, J., 1998. Climatología de la zona de Iquitos, Perú. Geoecol. Desarro. Amazon.: Estudio Integr. Zona Lquitos, Peru 35, 57.
McLauchlan, K.K., Higuera, P.E., Miesel, J., Rogers, B.M., Schweitzer, J., Shuman, J.K., Tepley, A.J., Varner, J.M., Veblen, T.T., Adalsteinsson, S.A., Balch, J.K., 2020. Fire as a fundamental ecological process: research advances and frontiers. J. Ecol. 108 (5), 2047–2069. https://doi.org/10.1111/1365-2745.13403.
Mertes, L.A., 1997. Documentation and significance of the perirheic zone on inundated floodplains. Water Resour. Res. 33 (7), 1749–1762. https://doi.org/10.1029/97WR00658.
Mix, A.C., Morey, A.E., 1996. Climate feedback and Pleistocene variations in the Atlantic south equatorial current. In: The South Atlantic. Springer, Berlin, Heidelberg, pp. 503–525. https://doi.org/10.1007/978-3-642-80353-6_26.
Moore, P.D., Bellamy, D.J., 1974. Peatlands (No. 553.21). Elek Science. https://doi.org/10.1007/978-1-4684-6291-3.
Moore, P.D., Webb, J.A., Collison, M.E., 1991. Pollen Analysis. Blackwell scientific publications.
Morley, R.J., 1981. Development and vegetation dynamics of a lowland ombrogenous peat swamp in Kalimantan Tengah, Indonesia. J. Biogeogr. 383–404. https://doi.org/10.2307/2844758.
Moutsamboté, J.M., 2012. Ecological, phytogeographic and phytosociological study of northern Congo (Plateaus, Bowls, Likouala and Sangha) (632 p. In: State Doctoral Thesis. University of Marien Ngouabi, Brazzaville.
Nakagawa, T., Brugiapaglia, E., Digerfeldt, G., Reille, M., Beaulieu, J.L.D., Yasuda, Y., 1998. Dense-media separation as a more efficient pollen extraction method for use with organic sediment/deposit samples: comparison with the conventional method. Boreas 27 (1), 15–24. https://doi.org/10.1111/j.1502-3885.1998.tb00864.x.
Ngomanda, A., Chepstow-Lusty, A., Makaya, M.V., Favier, C., Schevin, P., Maley, J., Fontugne, M., Oslisly, R., Jolly, D., 2009. Western equatorial African forest-savanna mosaics: a legacy of late Holocene climatic change? Clim. Past Discuss 5 (4). https://doi.org/10.5194/cp-5-647-2009.
Oksanen, J.F., Blanchet, G., Friendly, M., Kindt, R., Legendre, P., McGlinn, D., Minchin, P.R., O'Hara, R.B., Simpson, G.L., Solymos, P., Henry, M., Stevens, H., Szoecs, E., Wagner, H., 2020. vegan: Community Ecology Package. R package version 2.5-7. https://CRAN.R-project.org/package=vegan.
Olivero, J., Fa, J.E., Farfán, M.A., Lewis, J., Hewlett, B., Breuer, T., Carpaneto, G.M., Fernández, M., Germi, F., Hattori, S., Head, J., 2016. Distribution and numbers of Pygmies in central African forests. PLoS One 11 (1), e0144499. https://doi.org/10.1371/journal.pone.0144499.
Page, S.E., Rieley, J.O., Shotyk, Ø.W., Weiss, D., 1999. Interdependence of peat and vegetation in a tropical peat swamp forest. In: Changes and Disturbance in Tropical Rainforest in South-East Asia, pp. 161–173. https://doi.org/10.1142/9781848160125_0014.
Page, S.E., Rieley, J.O., Wüst, R., 2006. Lowland tropical peatlands of southeast Asia. Dev. Earth Surf. Process 9, 145–172. https://doi.org/10.1016/S0928-2025(06)09007-9.
Peck, J.A., Green, R.R., Shanahan, T., King, J.W., Overpeck, J.T., Scholz, C.A., 2004. A magnetic mineral record of Late Quaternary tropical climate variability from Lake Bosumtwi, Ghana. Palaeogeogr. Palaeoclimatol. Palaeoecol. 215 (1–2), 37–57. https://doi.org/10.1016/S0031-0182(04)00438-9.
Phillips, S., Rouse, G.E., Bustin, R.M., 1997. Vegetation zones and diagnostic pollen profiles of a coastal peat swamp, Bocas del Toro, Panama. Palaeogeogr. Palaeoclimatol. Palaeoecol. 128 (1–4), 301–338. https://doi.org/10.1016/S0031-0182(97)81129-7.
Pickett, S., Cadenasso, M.L., Meiners, S.J., 2009. Ever since Clements: from succession to vegetation dynamics and understanding to intervention. Appl. Veg. Sci. 9–21. https://doi.org/10.1111/j.1654-109X.2009.01019.x.
Prentice, I.C., 1985. Pollen representation, source area, and basin size: toward a unified theory of pollen analysis. Quat. Res. 23 (1), 76–86. https://doi.org/10.1016/0033-5894(85)90073-0.
Qing-feng, W., Zhi-yun, Z., Jia-kuan, C., 1997. Pollen morphology of the Alismataceae. J. Systemat. Evol. 35 (3), 225.
Quik, C., Palstra, S.W., van Beek, R., van der Velde, Y., Candel, J.H., van der Linden, M., Kubiak-Martens, L., Swindles, G.T., Makaske, B., Wallinga, J., 2022. Dating basal peat: the geochronology of peat initiation revisited. Quat. Geochronol., 101278
R Core Team, 2021. R: A Language and Environment for Statistical Computing. R Foundation for Statistical Computing, Vienna, Austria. https://www.R-project.org/.
Renssen, H., Goosse, H., Roche, D.M., Seppä, H., 2018. The global hydroclimate response during the Younger Dryas event. Quat. Sci. Rev. 193, 84–97. https://doi.org/10.1016/j.quascirev.2018.05.033.
Reynaud-Farrera, I., Maley, J., Wirrmann, D., 1996. Végétation et climat dans les forêts du Sud-Ouest Cameroun depuis 4770 ans BP: analyse pollinique des sédiments du Lac Ossa. CR Acad. Sci. Paris 322, 749–755 (série II a).
Roberts, D.W., 2019. Labdsv: Ordination and Multivariate Analysis for Ecology. R package version 2.0-1. https://CRAN.R-project.org/package=labdsv.
Roberts, N., Taieb, M., Barker, P., Damnati, B., Icole, M., Williamson, D., 1993. Timing of the younger dryas event in East Africa from Lake-level changes. Nature 366 (6451), 146–148. https://doi.org/10.1038/366146a0.
Roberts, M.E., Stewart, B.M., Tingley, D., 2019. Stm: an R package for structural topic models. J. Stat. Software (2), 1–40. https://doi.org/10.18637/jss.v091.i02, 10.18637/jss.v091.i02.
Roucoux, K.H., Lawson, I.T., Jones, T.D., Baker, T.R., Coronado, E.H., Gosling, W.D., Lähteenoja, O., 2013. Vegetation development in an Amazonian peatland. Palaeogeogr. Palaeoclimatol. Palaeoecol. 374, 242–255. https://doi.org/10.1016/j.palaeo.2013.01.023.
Rydin, H., Jeglum, J.K., Bennett, K.D., 2013. The Biology of Peatlands, vol. 2e. Oxford university press. https://doi.org/10.1093/acprof:osobl/9780199602995.001.0001.
Sachse, D., Billault, I., Bowen, G.J., Chikaraishi, Y., Dawson, T.E., Feakins, S.J., Freeman, K.H., Magill, C.R., McInerney, F.A., van der Meer, M.T.J., Polissar, P., Robins, R.J., Sachs, J.P., Schmidt, H.-L., Sessions, A.L., White, J.W.C., West, J.B., Kahmen, A., 2012. Molecular paleohydrology: interpreting the hydrogen-isotopic composition of lipid biomarkers from photosynthesizing organisms. Annu. Rev. Earth Planet Sci. 40, 221–249. https://doi.org/10.1146/annurev-earth-042711-105535.
Samba, G., Nganga, D., Mpounza, M., 2008. Rainfall and temperature variations over Congo-Brazzaville between 1950 and 1998. Theor. Appl. Climatol. 91 (1–4), 85–97. https://doi.org/10.1007/s00704-007-0298-0.
Schefuß, E., Schouten, S., Schneider, R.R., 2005. Climatic controls on central African hydrology during the past 20,000 years. Nature 437 (7061), 1003–1006. https://doi.org/10.1038/nature03945.
Sebag, D., Verrecchia, E.P., Cécillon, L., Adatte, T., Albrecht, R., Aubert, M., Bureau, F., Cailleau, G., Copard, Y., Decaens, T., Disnar, J.R., 2016. Dynamics of soil organic matter based on new Rock-Eval indices. Geoderma 284, 185–203. https://doi.org/10.1016/j.geoderma.2016.08.025.
Shackleton, N.J., 2000. The 100,000-year ice-age cycle identified and found to lag temperature, carbon dioxide, and orbital eccentricity. Science 289, 1897–1902. https://doi.org/10.1126/science.289.5486.1897.
Shanahan, T.M., McKay, N.P., Hughen, K.A., Overpeck, J.T., Otto-Bliesner, B., Heil, C.W., King, J., Scholz, C.A., Peck, J., 2015. The time-transgressive termination of the African Humid Period. Nat. Geosci. 8 (2), 140–144. https://doi.org/10.1038/ngeo2329.
Smith, F.A., Freeman, K.H., 2006. Influence of physiology and climate on δD of leaf wax n-alkanes from C3 and C4 grasses. Geochem. Cosmochim. Acta 70, 1172–1187. https://doi.org/10.1016/j.gca.2005.11.006.
Sowunmi, M.A., 1999. The significance of the oil palm (Elaeis guineensis Jacq.) in the late Holocene environments of west and west central Africa: a further consideration. Veg. Hist. Archaeobotany 8 (3), 199–210. https://doi.org/10.1007/BF02342720.
Stager, J.C., Mayewski, P.A., Meeker, L.D., 2002. Cooling cycles, Heinrich event 1, and the desiccation of Lake Victoria. Palaeogeogr. Palaeoclimatol. Palaeoecol. 183 (1–2), 169–178. https://doi.org/10.1016/S0031-0182(01)00468-0.
Swindles, G.T., Morris, P.J., Whitney, B., Galloway, J.M., Gałka, M., Gallego-Sala, A., Macumber, A.L., Mullan, D., Smith, M.W., Amesbury, M.J., Roland, T.P., 2018. Ecosystem state shifts during long-term development of an Amazonian peatland. Global Change Biol. 24 (2), 738–757. https://doi.org/10.1111/gcb.13950.
Tauber, H., 1967. Investigations of the mode of pollen transfer in forested areas. Rev. Palaeobot. Palynol. 3 (1–4), 277–286. https://doi.org/10.1016/0034-6667(67)90060-7.
Tierney, J.E., Russell, J.M., Damste, J.S.S., Huang, Y.S., Verschuren, D., 2011. Late quaternary behavior of the east African monsoon and the importance of the Congo air boundary. Quat. Sci. Rev. 30, 798–807. https://doi.org/10.1016/j.quascirev.2011.01.017.
Tierney, J.E., Pausata, F.S.R., deMenocal, P.B., 2017. Rainfall regimes of the green Sahara. Sci. Adv. 3, e1601503. https://doi.org/10.1126/sciadv.1601503.
Tovar, C., Harris, D.J., Breman, E., Brncic, T., Willis, K.J., 2019. Tropical monodominant forest resilience to climate change in Central Africa: a Gilbertiodendron dewevrei forest pollen record over the past 2,700 years. J. Veg. Sci. 30 (3), 575–586. https://doi.org/10.1111/jvs.12746.
van der Valk, A.G., 1981. Succession in wetlands: a gleasonian approch. Ecology 62 (3), 688–696. https://doi.org/10.2307/1937737.
Veenendaal, E.M., Torello-Raventos, M., Miranda, H.S., Sato, N.M., Oliveras, I., van Langevelde, F., Asner, G.P., Lloyd, J., 2018. On the relationship between fire regime and vegetation structure in the tropics. New Phytol. 218 (1), 153–166. https://doi.org/10.1111/nph.14940.
Vellend, M., 2010. Conceptual synthesis in community ecology. Q. Rev. Biol. 85 (2), 183–206. https://doi.org/10.1086/652373.
Vimeux, F., Masson, V., Delaygue, G., Jouzel, J., Petit, J.R., Stievenard, M., 2001. A 420,000 year deuterium excess record from East Antarctica: information on past changes in the origin of precipitation at Vostok. J. Geophys. Res. 106, 31863–31873. https://doi.org/10.1029/2001JD900076.
Vincens, A., Buchet, G., Elenga, H., Fournier, M., Martin, L., de Namur, C., Schwartz, D., Servant, M., Wirrmann, D., 1994. Changement majeur de la végétation du lac Sinnda (vallée du Niari, Sud-Congo) consécutif à l'assèchement climatique holocène supérieur: apport de la palynologie. Compt. Rendus à l'Acad. Sci. Paris 318, 1521–1526.

Vincens, A., Schwartz, D., Elenga, H., Reynaud-Farrera, I., Alexandre, A., Bertaux, J., Mariotti, A., Martin, L., Meunier, J.D., Nguetsop, F., Servant, M., 1999. Forest response to climate changes in Atlantic Equatorial Africa during the last 4000 years BP and inheritance on the modern landscapes. J. Biogeogr. 26, 879–885.

Vincens, A., Dubois, M.A., Guillet, B., Achoundong, G., Buchet, G., Beyala, V.K.K., De Namur, C., Riera, B., 2000. Pollen-rain-vegetation relationships along a forest-savanna transect in southeastern Cameroon. Rev. Palaeobot. Palynol. 110 (3–4), 191–208. https://doi.org/10.1016/S0034-6667(00)00009-9.

Vincens, A., Bremond, L., Brewer, S., Buchet, G., Dussouillez, P., 2006. Modern pollen-based biome reconstructions in East Africa expanded to southern Tanzania. Rev. Palaeobot. Palynol. 140, 187–212. https://doi.org/10.1016/j.revpalbo.2006.04.003.

Waelbroeck, C., Labeyrie, L., Michel, E., Duplessy, J.C., McManus, J.F., Lambeck, K., Balbon, E., Labracherie, M., 2002. Sea-level and deep water temperature changes derived from benthic foraminifera isotopic records. Quat. Sci. Rev. 21, 295–305. https://doi.org/10.1016/S0277-3791(01)00101-9.

Weijers, J.W., Schefuß, E., Schouten, S., Damsté, J.S.S., 2007. Coupled thermal and hydrological evolution of tropical Africa over the last deglaciation. Science 315 (5819), 1701–1704. https://doi.org/10.1126/science.1138131.

Whitney, B.S., Smallman, T.L., Mitchard, E.T., Carson, J.F., Mayle, F.E., Bunting, M.J., 2019. Constraining pollen-based estimates of forest cover in the Amazon: a simulation approach. Holocene 29 (2), 262–270. https://doi.org/10.1177/0959683618810394.

Young, D.M., Baird, A.J., Gallego-Sala, A.V., Loisel, J., 2021. A cautionary tale about using the apparent carbon accumulation rate (aCAR) obtained from peat cores. Sci. Rep. 11 (1), 1–12. https://doi.org/10.1038/s41598-021-88766-8.